ROUGH SURFACE PREPARATION THROUGH CHEMICAL ETCHING FOR SUPER-HYDROPHOBICITY

AISSWARYA KUMARAN

FACULTY OF ENGINEERING

UNIVERSITY OF MALAYA

KUALA LUMPUR

2016

ROUGH SURFACE PREPARATION THROUGH CHEMICAL ETCHING FOR SUPER-HYDROPHOBICITY

AISSWARYA KUMARAN

RESEARCH REPORT SUBMITTED TO THE FACULTY OF ENGINEERING UNIVERSITY OF MALAYA, IN PARTIAL FULFILLMENT OF THE REQUIREMENTS FOR THE DEGREE OF MASTERS OF ENGINEERING (MECHANICAL)

FACULTY OF ENGINEERING
UNIVERSITY OF MALAYA
KUALA LUMPUR

2016

UNIVERSITY OF MALAYA
ORIGINAL LITERARY WORK DECLARATION

Name of Candidate: Aisswarya Kumaran

Matric No: KGY140020

Name of Degree: Masters in Engineering (Mechanical)

Title of Project Paper/Research Report/Dissertation/Thesis ("this Work"):

Rough Surface Preparation Through Chemical Etching for Super-Hydrophobicity

Field of Study:

Heat Transfer/Surface Engineering

I do solemnly and sincerely declare that:

(1) I am the sole author/writer of this Work;
(2) This Work is original;
(3) Any use of any work in which copyright exists was done by way of fair dealing and for permitted purposes and any excerpt or extract from, or reference to or reproduction of any copyright work has been disclosed expressly and sufficiently and the title of the Work and its authorship have been acknowledged in this Work;
(4) I do not have any actual knowledge nor do I ought reasonably to know that the making of this work constitutes an infringement of any copyright work;
(5) I hereby assign all and every rights in the copyright to this Work to the University of Malaya ("UM"), who henceforth shall be owner of the copyright in this Work and that any reproduction or use in any form or by any means whatsoever is prohibited without the written consent of UM having been first had and obtained;
(6) I am fully aware that if in the course of making this Work I have infringed any copyright whether intentionally or otherwise, I may be subject to legal action or any other action as may be determined by UM.

Candidate's Signature Date:

Subscribed and solemnly declared before,

Witness's Signature Date:

Name:

Designation:

ABSTRACT

Super-hydrophobic films with water contact angle higher than 150° have been the subject of great interest and enthusiastic study in recent years. These films are fabricated by incorporating appropriate surface roughness with surfaces of low surface energy. The interest in surfaces with self-cleaning ability is being driven by its various applications. In this project, superhydrophobic surface was produced through chemical etching process using myristic acid and ethanol solution of hydrochloric acid. Few parameters, namely etching time, myristic acid concentration, type of aluminium substrate in terms of thickness and reaction temperature were manipulated to determine which is optimum. The resultant contact angle was measured using an optical angle meter to determine if the superhydrophobic state has been achieved. The surface morphology and chemical composition was examined using SEM and EDS respectively. Subsequently, the highest contact angle achieved was 159.4º±1.1º. The end-product surface showed micro-nano morphology, which is a significant characteristic of superhydrophobic surface. EDS results indicated the formation of aluminium palmitate due to the bonding between tetradecanoate ion, $CH_3(CH_2)_{12}COO^-$ with the Al^{3+} on the aluminium surface. Calculations revealed that 95.2% of the surface area is made up of solid-air interface, implying that only 4.8% of the surface is in contact with the water droplet. This method for fabrication of superhydrophobic surface can be used for large-scale fabrication of superhydrophobic Al surfaces as technique is low-cost, quick and simple to adopt.

ABSTRAK

Filem super-hidrofobik dengan sudut sentuhan air yang lebih tinggi daripada 150 ° telah menjadi subjek minat dan kajian popular dalam beberapa tahun kebelakangan ini. Filem-filem ini adalah direka dengan menggabungkan ciri kekasaran permukaan yang sesuai dengan permukaan tenaga permukaan rendah. Dalam projek ini, permukaan superhydrofobik telah dihasilkan melalui proses punaran kimia menggunakan asid Myritic dan larutan asid etanol hidroklorik. Beberapa pemboleh ubah seperti masa punaran, konsentrasi asid Myritic, jenis substrat aluminium dari segi ketebalannya dan suhu tindak balas telah dimanipulasikan untuk menentukan mana yang optimum. Sudut sentuhan air diukur menggunakan meter sudut optik untuk menentukan sama ada keadaan superhydrofobik telah dicapai. Morfologi permukaan dan komposisi kimia telah diperiksa menggunakan SEM dan EDS. Hasilnya, sudut sentuhan air tertinggi yang dicapai adalah 159.4º ± 1.1º. Permukaan produk akhir menunjukkan morfologi mikro-nano, yang merupakan ciri-ciri yang ketara pada permukaan superhydrofobik. Keputusan EDS menunjukkan pembentukan kompaun *palmitate aluminium* kerana ikatan antara ion tetradecanoate, $CH_3(CH_2)_{12}COO^-$ dengan Al^{3+} pada permukaan aluminium. Pengiraan dan analisa menunjukkan bahawa 95.2% daripada kawasan permukaan terdiri daripada antara muka pepejal dengan udara, menunjukkan bahawa hanya 4.8% daripada permukaan bersentuhan dengan titisan air. Kaedah ini untuk menghasilkan permukaan superhydrofobik boleh digunakan untuk fabrikasi berskala besar permukaan Al yang tidak dibasahi oleh air sebab teknik ini adalah kos rendah, cepat dan mudah untuk diaplikasi.

ACKNOWLEDGEMENT

My grateful appreciation goes to everyone who has assisted me directly and indirectly throughout the course of this project. I express my sincere gratitude to my supervisor Dr Poo Balan Ganesan for his guidance, advice and mentoring throughout this project. Under his supervision I have gained a lot of valuable knowledge and experience in the area of scientific research and academic writing.

I would also like to express my gratitude to the staff of Tissue Engineering Laboratory and Biomedical Engineering for their kind assistance throughout the experiments conducted for this project. Special thanks to my colleague Mr Ganan whom provided assistance on numerous occasions during the duration of laboratory works, knowledge-sharing as well as the handling of scientific equipment.

Besides that, my sincere appreciation to my family and friends for their support, encouragement, faith in me and morale boost to continue in the pursuit of my dreams. Besides that, I would like to extend my appreciation to my other post-graduate friends, Mr Manoj and Arafat who made me feel welcome into this research group and have been there for me in times of need. Last but not least, I would like to thank MyBrian15 for supporting my postgraduate education in University of Malaya.

TABLE OF CONTENTS

ABSTRACT ii
ABSTRAK iii
ACKNOWLEDGEMENT iv
LIST OF FIGURES vii
LIST OF TABLES viii
CHAPTER 1 1
INTRODUCTION 1
1.1 BACKGROUND OF STUDY 1
1.1.1 Surface Wettability and Contact Angle 2
1.2 PROBLEM STATEMENTS 3
1.3 OBJECTIVES OF RESEARCH 4
1.3.1 Specific Objectives 4
1.4 THESIS OUTLINE 5
CHAPTER 2 7
LITERATURE REVIEW 7
2.1 OVERVIEW 7
2.2 INTRODUCTION 7
2.3 WETTABILITY MODELS 8
2.3.1 Wenzel Model 8
2.3.2 Cassie-Baxter Model 9
2.3.3. Mamur Model 9
2.4 CONTACT ANGLE MEASUREMENT TECHNIQUES 10
2.5 FABRICATION OF SURFACE ROUGHNESS FOR SUPERHYDROPHOBICITY 11
2.5.1 Hierarchical Structures and Nanoparticles 12
2.5.2 Development years 13
2.6 BASE MATERIALS 14
2.7 METHOD OF ROUGH SURFACE PREPARATION 18
2.8 SURFACE MORPHOLOGY AND SHAPES 22
2.9 LOW SURFACE ENERGY COATING MATERIALS 25
2.10 CONTACT ANGLE AND ROLL-OFF ANGLE ACHIEVED 29
2.11 DURABILITY OF SURFACE AND POTENTIAL APPLICATIONS 31

CHAPTER 3 34
METHODOLOGY 34
3.1 OVERVIEW 34
3.2 MATERIALS 36
3.3 SAMPLE PREPARATION AND EXPERIMENTATION 37
3.3.1 Effect of Different Etching Time on Superhydrophobicity 37
3.3.2 Effect of Myristic Acid Concentration on Superhydrophobicity 37
3.3.3 Effect of Type of Aluminium Substrates on Superhydrophobicity 38
3.3.4 Influence of Reaction Temperature on Superhydrophobicity 38
3.4 WETTABILITY MEASUREMENTS, SURFACE COMPOSITION AND MORPHOLOGY ANALYSIS 42
3.4.1 Wettability Measurements 42
3.4.2 Surface Morphology and Composition Analysis 42
CHAPTER 4 45
RESULTS AND DISCUSSION 45
4.1 OVERVIEW 45
4.2 EFFECT OF DIFFERENT ETCHING TIMES ON SUPERHYDROPHOBICITY 45
4.3 INFLUENCE OF MYRISTIC ACID (MYA) CONCENTRATION ON SUPERHYDROPHOBICITY 48
4.4 INFLUENCE OF DIFFERENT TYPES OF ALUMINIUM SUBSTRATE ON SUPERHYDROPHOBICITY 51
4.5 EFFECT OF VARIOUS REACTION TEMPERATURES ON SUPERHYDROPHOBICITY 52
4.6 MYRISTIC ACID AND HYDROCHLORIC ACID IN ETHANOL SOLUTION AS ETCHANT 56
4.6.1 Chemical Reactions during modification and formation of Superhydrophobic Surface 57
4.7 WETTABILITY ANALYSIS OF SHP SURFACE 59
4.8 EDS ANALYSIS 60
CHAPTER 5 63
CONCLUSION 63
REFERENCES 65
APPENDIX A 76

LIST OF FIGURES

Figure 2.1: The different wetting states of liquid droplet on rough surface 10
Figure 2.2: Development years in the field of super-liquid-repellant surface research . 13
Figure 2.3: Various base materials used for superhydrophobic surface research 16
Figure 2.4: Types of metals used as base substrates 17
Figure 2.5: Methods of rough surface fabrication 19
Figure 2.6: Surface Morphology and Microstructure 23
Figure 2.7: Low surface energy coating materials 26
Figure 2.8: Water droplet mobility in terms of contact angle and sliding angle 29
Figure 3.1: Summary of Experimental Procedures 35
Figure 3.2: Aluminum fin sample of thickness 0.1 mm 36
Figure 3.3: Aluminum foil with thickness of 0.2 mm 36
Figure 3.4: Aluminum plate with thickness of 1.5 mm 37
Figure 3.5: Aluminium foil immersed into etchant solution 39
Figure 3.6: Experimental set-up to heat etchant and substrate using laboratory heater . 39
Figure 3.7: OCA 15EC optical angle meter to measure water contact angle 43
Figure 3.8: Hitachi model SU8220 field-emission scanning electron microscopy (FE-SEM) with EDS 44
Figure 4.1: Effect of etching time on water contact angle 46
Figure 4.2: SEM image of sample etched for 10 minutes producing CA = 145.6±1.3º 47
Figure 4.3: SEM image of sample etched for 15 minutes producing CA = 159.4±1.1º 47
Figure 4.4: SEM image of sample etched for 20 minutes producing CA = 157.8±0.5º 48
Figure 4.5: Effect of myristic acid concentration on water contact angle 49
Figure 4.6: Contact angle and sliding angle versus different concentrations of stearic acid (STA) adapted from Rezayi & Entezari (2016) 50
Figure 4.7: Effect of type of aluminium substrate in terms of thickness on water contact angle 52
Figure 4.8: Effect of temperature on water contact angle 53
Figure 4.9: Sample J etched subject to reaction temperature of 50°C 54
Figure 4.10: Sample N etched subject to reaction temperature of 70°C 54
Figure 4.11: Sample P etched subject to reaction temperature of 80°C 55
Figure 4.12: Illustration of superhydrophobic surface preparation on Al substrates using the single-step process adapted from Zhang et al. (2011) 59
Figure 4.13: EDS results of bare Al3102 fin 61
Figure 4.14: EDS results of sample B with CA =159.4º±1.1º 62

LIST OF TABLES

Table 2.1: Other commonly used surface roughness preparation methods.....22
Table 2.2: Papers with micro-level surface morphology 25
Table 3.1: Simulation cases of parameters for experiments 1-4 41
Table 4.1 : Contact angle values for various etching times 46
Table 4.2: Contact angle values for different myristic acid concentrations.....48
Table 4.3: Contact angle values for different types of aluminium substrate.....51
Table 4.4: Contact angles measured on silver surfaces patterned with 5.5µm microspheres using NSL covered with SAM of 1H,1H,2H,2H-Perfluorodecanethiol adapted from Pacifico et al. (2006) 52
Table 4.5: Contact angle values for samples subject to different reaction temperatures53
Table 4.6: EDS results of bare aluminium sample and treated superhydrophobic sample B 61

LIST OF SYMBOLS AND ABBREVIATIONS

°C	Degree Celcius
ml	millilitre
θ	Theta
r	Material roughness
f	Fraction
θ_{adv}	Advancing angle
θ_{rec}	Receding angle
mg	Milligram
g	Gram
g/l	Gram Per Liter
DCA	Dynamic contact angle
L	Liters
CA	Contact angle
SA	Sliding angle
µm	Micrometre
nm	Nanometre
°	Degree
SiO_2	Silicon dioxide
SEM	Scanning electron microscopy
mN/m	Millinewton/meter
mL/s	Millilitre/second
EDS	Energy dispersive spectroscopy
HCl	Hydrochloric acid

$CH_3(CH_2)_{12}COOH$	Myristic acid
mm	Millimetre
mins	minutes
µL	Microlitre
CAH	Contact angle hysteresis
FE-SEM	Field-emission scanning electron microscopy
f_a	Area ratio of air and solid surface
f_s	Area ratio of solid that contacts water
$Al(CH_3(CH_2)_{12}COO)_3$	Aluminium palmitate
Cl^-	Chloride ions
H^+	Hydrogen ions
Al^{3+}	Aluminium ion
Al	Aluminium
$AlCl_3$	Aluminium chloride
H_2	Hydrogen
H_2O	Water
O_2	Oxygen
$CH_3(CH_2)_{12}COO^-$	Tetradecanoate ion
θ_{rough}	Contact angle of rough surface after chemical etching
θ_{flat}	Contact angel on flat bare aluminium sample before treatment
O	Oxygen
C	Carbon
Si	Silicon
H_2	Hydrogen
Fe	Iron
wt%	Percentage weight

CHAPTER 1

INTRODUCTION

1.1 BACKGROUND OF STUDY

Superhydrophobic films with water contact angle higher than 150° have been the subject of great interest and enthusiastic study in recent years. These films are fabricated by incorporating appropriate surface roughness with surfaces of low surface energy. Many surfaces in nature are highly hydrophobic and self-cleaning such as the lotus leaf, the wings of butterflies and the leaves of plants such as cabbage and Indian cress. Controlling surface wettability is an important consideration relevant to many areas of technology.

The interest in surfaces with self-cleaning ability is being driven by its various applications such as satellite dishes, solar energy panels, photovoltaics, exterior architectural glass and green houses, and heat transfer surfaces in air conditioning equipment. Non-wettable surfaces also have the ability to prevent frost from forming or adhering to the surface. The fact that liquid in contact with such a surface slides with lowered friction suggests relevance for microfluidics, piping and boat hulls. The non-wettable character has been asserted in biomedical applications ranging from blood vessel replacement to wound management.

This research focuses on the mobility of water droplet on superhydrophobic surface and how factors such as surface roughness, coating material and temperature play a role in anti-wetting property. Laboratory scale test rigs were produced to observe mobility in terms of water contact angle, sliding angle (SA), advancing angle, receding angle and contact angle hysteresis (CAH). Optimization testing was conducted to

determine the parameters and cost-efficient methodologies which enable the highest superhydrophobicity.

1.1.1 Surface Wettability and Contact Angle

Contact angle (CA) of liquid specifies its wettability, i.e. whether or not the liquid comes into close proximity with the surface it is lying on. Contact angle is described as the computable angle that a liquid makes with a solid and indicates where a liquid–vapour interface meets a solid surface. When the value of CA is $0 \leq \theta \leq 90$, the liquid will wet the surface (referred to as non-wetting liquid and hydrophilic surface), while at CA values between 90 to 180, the liquid does not wet the surface (in this case it is classified as wetting liquid and hydrophobic surface).

Surfaces with CA values of ~ 0 and within the range of 150 – 180 are known as superhydrophilic and superhydrophobic respectively (Nosonovsky & Bhushan, 2007). Super-hydrophobic films, originally inspired by the one-of-a-kind water repellent characteristic of the lotus leaf, have been the subject of great interest and enthusiastic study in recent years. Technologies related to superhydrophobic coatings are deemed to be significant for restraining chemical reactions and bond formation between water and solid surfaces.

These coatings have various application including prevention of snow, fog and raindrops adhesion to antennas and windows; reduction of friction resistance; anticontaminant and antioxidation micro fluids (Li et al., 2005 & Shi et al., 2012). Due to research and development advancements in this area, it is forecasted that super-hydrophobic surfaces with micro/nano-structures will be used in the fields of national defence, industrial and agricultural production and human daily life widely (such as soil-repellent garments according to Liu et al. (2016).

1.2 PROBLEM STATEMENTS

In air-conditioning systems, which using the fin-and-tube heat exchangers, condensation of moisture occurs when the surface temperature is below the dew point of the conditioned air. This moisture accumulates on the fins of the evaporator or cooling coil. As the quantity of condensed water on fin surfaces increases, gravitational or airflow forces drag some droplets downward, while surface tension cause remaining droplets to adhere to the surface (termed as "water hold-up").

According to a review by Ganesan et al. (2016), the adherence of water beads on fins results in several undesirable phenomena inside the heat exchangers such as (i) bridging between fins, increasing air-side pressure drop; (ii) air-side heat transfer coefficient is decreased; (iii) demeaning of cooling capacity; (iv) corrosion; (v) creating a moist environment conducive for biological activity.

Furthermore, another predicament in fins surfaces is the development of frost layers when subject to winter conditions. This affects heat exchanger performance due to several reasons namely increase of heat transfer resistance between the fin and airflow, obstruction of airflow pathways within fins and shutdown of heat pumps. Hence, it can be said that an efficient defrosting process is necessary to melt the frost layer.

Most evaporators used in heating, ventilation and air-conditioning (HVAC) systems have hydrophilic coatings, which increases the surface wettability (reduces the liquid condensate contact angle). Besides that, the film wise condensate layer (formed when the condensate forms a film that covers the solid surface) is thinner. As the result of both these phenomena, the fan power consumption is lessened. Despite this event, along with the advantage of lower aerodynamic noise level at fixed air velocity for the

same pressure drop, hydrophilic surface treatment adds to thermal resistance, which is not desirable for heat exchanger.

Correspondingly, an ingenious design with surface treatment for water retention minimization and frost layer retardation is required to enhance the heat transfer efficiency of finned-and-tube heat exchanger. Ultimately, the outcome of this research in this area would be smaller, lighter, quieter and energy-saving systems.

1.3 OBJECTIVES OF RESEARCH

The main aim of this research is to examine the potential of surface roughness created by chemical etching in increasing the super hydrophobicity of aluminium sample to enhance its anti-wetting properties to be applied in heat exchangers and air conditioning fins for anti-icing applications.

1.3.1 Specific Objectives

The specific objectives of this project are :

1. To determine the most optimum etching parameters, which induce surface non-wettability and achieve hydrophobic and superhydrophobic states when etching using ethanol solution of hydrochloric acid and myristic acid.
2. To investigate whether the one-step etching process can produce contact angle (CA) above 150^{o} and similar surface chemical composition and morphology as when traditional two-step etching is done.

1.4 THESIS OUTLINE

This thesis format is as follows: Introduction, Literature Review, Methodology, Results and Discussion, and Conclusion. A brief summary for each chapter is shown below:

Chapter 1: Introduction

In this chapter a brief overview of the project is stated. Next, the research background of this project is explained. The problem statements and objectives of this research are also specified in this section.

Chapter 2 : Literature Review

Literature Review describes wettability models, contact angle measurement techniques, fabrication of roughness-induced superhydrophobic surfaces, types of base materials used as substrates, method of rough surface preparation, surface morphology and shapes, rough surface coating contact and roll-off angle achieved in previous works, durability and potential applications of the fabricated surfaces. This chapter will discuss previous research in these areas.

Chapter 3 : Methodology

This chapter reports the research methodology for this project. The materials used, sample preparation and experimentation methods are reviewed in this chapter. Additionally, wettability measurement techniques, surface composition and morphology analysis are explained in detail.

Chapter 4 : Results and Discussion

This chapter reviews the results of the experiments performed for this project in terms of how varying etching times, myristic acid quantity, type of substrate and reaction time influenced water contact angle. The trends obtained in each experiment's results are

clearly explained with proper scientific justification with reference to other researchers work. The results were tabulated in tables and graphical illustrations. SEM and EDS results were also examined and analysed.

Chapter 5 : Conclusion

This chapter sums up this project and affirms the key findings of this research.

CHAPTER 2

LITERATURE REVIEW

2.1 OVERVIEW

This chapter presents a review of rough surface preparation to develop a super-hydrophobic surface. In particular, a summary of details of base materials, methods of rough surface preparation, surface coating methods and materials, and the achieved surface contact angle including roll-off angle is provided. For some of the methods and techniques, the durability and the potential applications are provided.

2.2 INTRODUCTION

A solid surface which is conducive to water repellence is vital in daily life, industry and agriculture. According to Liu et al. (2007) & Bhushan et al. (2009), much research on this area has been inspired by naturally occurring surfaces in nature such as the superhydrophobic lotus leaf which possess waxy coating as well as nano-hairs on micro protrusions (dual scale micro/-nanostructures).

As the wetting or de-wetting feature of solid materials is governed by both surface roughness and chemical composition, enhancing surface roughness and lowering surface free energy are the two key points to be considered to increase hydrophobicity (Koch et al., 2009). Hence, the common strategies used for the creation of water-repellent surfaces is either by creating textured/rough structure on an inherent hydrophobic surface or modifying a rough surface with low surface free energy compounds by chemical means.

2.3 WETTABILITY MODELS

According to Park et al. (2011), the contact angle of a droplet on a flat surface is verified using Young's equations by equalized surface tensions at the solid liquid-air interface. This force balance method is equal to the local Gibbs free energy minimization at $dG/dx = 0$ at the three-phase interface (Ishino et al., 2004). Once the surface is no longer flat, introducing roughness, the contact angle is analyzed using Wenzel or Cassie-Baxter models based on surface chemical property.

2.3.1 Wenzel Model

The Wenzel and Cassie-Baxter models are two important examples commonly used to describe how surface roughness influences the apparent contact angle of a liquid droplet on a solid surface (Valipour et al., 2014). Both these concepts were derived under the assumption that the surface contains homogenous asperities and the period of these asperities is relatively smaller than the droplet radius.

Under the Wenzel condition established in 1936, the entire solid surface and liquid comes into contact and thoroughly diffuse into cavities as seen in Figure 2.1a. This model is applied for hydrophilic surfaces such that the liquid bead penetrates into the rough edges and comes into full contact with the surface (Kwon et al., 2009) and states that the surface area is greater for a rough surface compared to a smooth one, hence the CA is given by the following expression:

$\text{Cos } \theta^* = r \cos \theta$ ---------- Equation 2.1

Where θ^* is the apparent CA of liquid droplet on the rough surface, θ is the equilibrium CA on the smooth surface of the same material that can be described by Young's equation and r is the material's roughness which is the actual area divided by its flat projected area.

2.3.2 Cassie-Baxter Model

In year 1944, Cassie and Baxter proposed that liquid droplet cannot actually penetrates into these rough surface cavities as stated in the Wenzel model due to the presence of air in this cavities creating a composite interface (Motlagh et al., 2013). Thus, the droplet is merely positioned on the trapped air layer instead of the solid surface itself (Figure 2b). The Cassie-Baxter model is considered when estimating the CA on a super hydrophobic surface. The proposed equation for this model is as follows:

$$\text{Cos } \theta^* = f_1 \text{ Cos } \theta - f_2 \quad \text{Equation 2.2}$$

Where f_1 is the fraction of the liquid droplet area in contact with the solid surface and f_2 is the area fraction of the liquid drop in contact with the trapped air in the pores of the rough surface, and $f_1 + f_2 = 1$.

2.3.3. Mamur Model

Marmur introduced a mixed model where the droplet partly sits on the trapped air pockets and partly wets the solid surface as observed in Figure 2c. Thus, the surface CA is modified according to the equation :

$$\text{Cos } \theta^* = r_f f_{SL} \cos \theta + f_{SL} - 1 \quad \text{Equation 2.3}$$

where r_f is the roughness of the portion of the solid that touches the liquid and f_{SL} is the area fraction of the liquid droplet in contact with the solid surface.

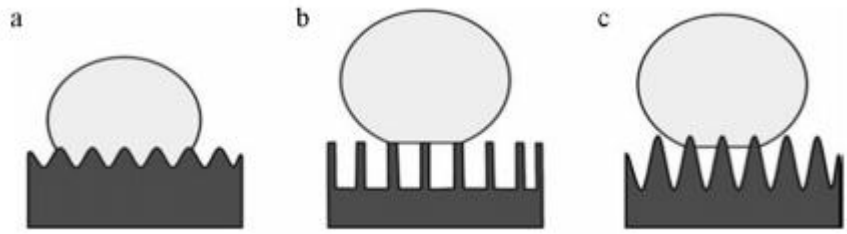

Figure 2.1: The different wetting states of liquid droplet on rough surface: (a) Wenzel state (b) Cassie-Baxter state and (c) Marmur state adapted from Valipour et al. (2014)

2.4 CONTACT ANGLE MEASUREMENT TECHNIQUES

The most widely used technique of contact angle measurement is a direct measurement of the tangent angle θ on a static drop profile by using "telescope-goniometer" also known as the *sessile drop method*. The phenomenon of wetting is more than just a static state. The liquid droplets form on the fin surface move via gravity and also the air going through the heat exchanger (at high airflow rates) (Sommers et al., 2012). When the droplets start to move, they advance over previously dry surface but recede from previously wet surface. This will create an advancing angle (θ_{adv}) and a receding angle (θ_{rec}).

Gokhale et al. (2003) conducted experimental observations reveal that as the rate of condensation increases, the contact angle increases. This means that a dynamic contact angel (DCA) should be considered in dropwise condensation. Dynamic contact angles are measured by using two common methods: (a) volume changing method and (b) tilted plate.

In the first method, water droplets are injected onto the surface of the fin using high-precision micro-syringe. The advancing and receding angles are then measured by increasing or decreasing the volume of water droplets injected on the surface until the maximum or minimum volume is achieved without a change in the droplet contact area. In the second method, the droplet is placed onto the surface, which is then gradually

tilted, and the measurement of θ_{adv} and θ_{rec} is performed just before the droplet starts to move.

The sliding angle (SA) is defined as the critical angle whereby a water droplet having a particular weight begins to glide down a tilted plane (Korhonen et al., 2013). The difference between the advancing and receding angle values indicate the contact angle hysteresis (CAH), which does not reflect any physical quantity. A study by Krasovitski & Marmur (2005) has proven that the size of the liquid droplet and type of surface roughness/morphology highly influence the sliding angle.

As stated by Valipour et al. (2014), measuring the sliding angle examines the roll-off behavior and self-cleaning characteristic of the surface. A simple methodology is used to measure the SA, whereby a droplet is placed on a surface, which is then slowly titled. Subsequently the SA is measured once the drop starts to move forward. High CA affirms liquid repellence by the solid surface, while low SA or CAH exhibits that the liquid has low adhesion to a solid enabling it to easily flow with low-energy dissipation, thus revealing its self-cleaning characteristic (Nosonovsky & Bhushan, 2007).

2.5 FABRICATION OF SURFACE ROUGHNESS FOR SUPERHYDROPHOBICITY

Surface roughness is an essential parameter with the ability to enhance hydrophobic properties (Wenzel, 1949 & Shang et al., 2005) and the two important conditions for the fabrication of super hydrophobic surfaces are appropriate surface roughness and low surface energy (Ma et al., 2006). As such, techniques to prepare a superhydrophobic surface can be classified according to two categories: (a) producing a

rough surface from a low-surface-energy material or (b) altering a rough surface with a low-surface-energy material.

Literature by Shi et al. (2012) states for category (a), low surface energy materials, namely fluorocarbons, silicones, organic materials (polyethylene, polystyrene, etc.) and inorganic materials (ZnO and TiO_2) are used to produce superhydrophobic surfaces. Category (b) is deemed as suitable for assorted hydrophilic substrates (such as silanes), which are required to feature a high roughness prior to its low-surface-energy material conversion.

Methods of rough surface fabrication are diversified including mechanical stretching, laser/plasma/chemical etching, lithography, sol–gel processing and solution casting, layer-by-layer and colloidal assembling, electrical/chemical reaction and deposition, electrospinning and chemical vapor deposition (Nimittrakoolchai & Supothina, 2008).

2.5.1 Hierarchical Structures and Nanoparticles

Research by Zhu et al. in year 2006 revealed that both the nanostructure and microstructure of a surface supplement superhydrophobicity. In 2007, studies by Hong et al. deduced that the hydrophobicity of many surfaces found in nature are caused by their hierarchical or multi-scale surface roughness at micro and nano scales (particularly at ca. 3-10μm and about 100 nm length scales) (i.e. nanoscale bumps superimposed over microscale asperities).

In recent times, surface roughening has been carried out via nanoparticles to achieve superhydrophobicity using two types of procedure. The first method was depositing nanoparticles on smooth or micro roughened substrates to generate substrates with submicron-scale surface roughness (Zhai et al., 2004; Bravo et al., 2007; Bok et al., 2008).

Subsequently, the substrates went through chemical treatment with low-surface-energy coatings to improve its hydrophobicity. In experiments by Hsieh et al. (2005), Chibowski et al. (2006) and Yuce et al. (2008), a mixture of nanoparticles and polymer solutions were deposited on smooth surfaces such as glass and silicon.

2.5.2 Development years

Referring to Figure 2.2, prior to year 2005, there is very limited research has been done. For last 10 years, there is a growing interest on creating super-hydrophobic surface based on rough surface creation. In particular, there is a significant increase in this research area in 2009. Since then, there is a steady and slow increase in number of researches has been done.

There is a sudden boost in interest towards this area among researchers starting from year 2015 onwards as there is an increasing trend as seen in the Figure 2.2. In year 2015, there are about 16 publications reporting experimental work on superhydrophobicity induced by textured surface morphology. Within the first few months of 2016 only, four studies have been already reported.

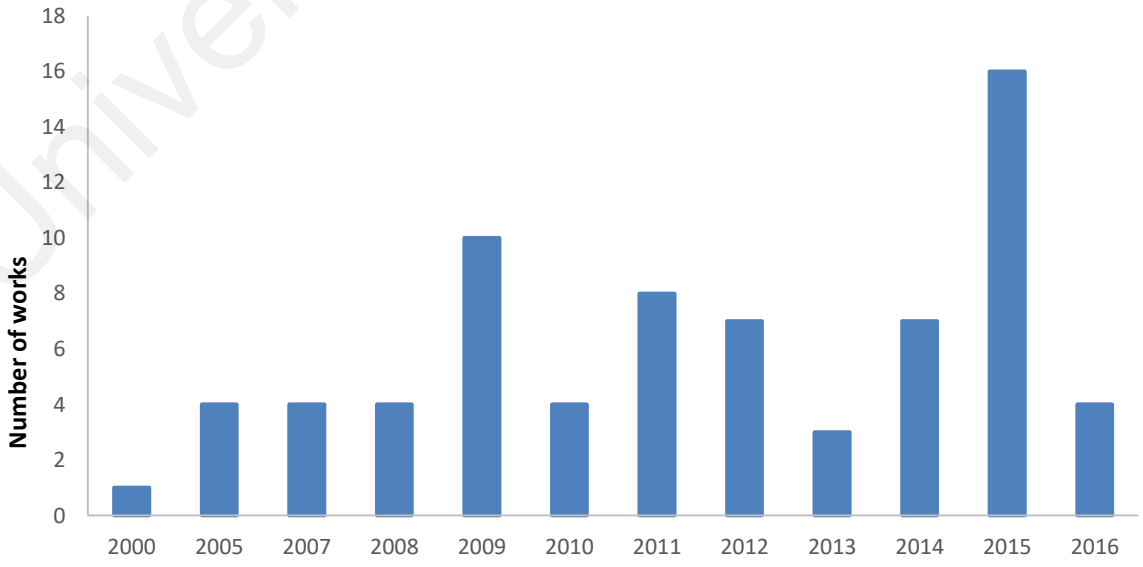

Figure 2.2: Development years in the field of super-liquid-repellent surface research

2.6 BASE MATERIALS

Substrate selection is the preliminary step taken prior to experiment in this research area. Various categories of base materials have been considered by researchers, namely metal, non-metal/others, fibrous, semi-metal, polymer and combination of any of the mentioned materials. Types of non-metal include glass substrate (Nakajima et al., 2000; Li et al., 2005; Shang et al., 2005; Nimittrkolchai &Supothina, 2008; Lakshmi & Basu, 2009; Mahadik et al., 2010; Park et al., 2011; Lakshmi et al., 2012; Lathe & Rao, 2012; Tian et al., 2015), sapphire wafer (Wang et al., 2009) and sand paper of different grid sizes creating a variety of rough/coarse surfaces (Das et al., 2012).

Fibrous materials comprising of natural fiber tissues originating from annual plants tissues exhibit excellent mechanical properties and functional behavior (Koh et al., 2015). Examples of fibrous materials used as substrates for the fabrication of superhydrophobic surfaces are cotton fabrics (Yu et al., 2007; Berendjchi et al., 2011; Charyangi et al., 2016), pristine poplar wood (Wang et al., 2011 & Fu et al., 2012) and eucalyptus wood (Liu et al., 2015c). In 2009, researchers led by Yoon et al. used fibrous cellulose triacetate (CTA) mats.

The only semi-metal substrate contemplated is silicon (Hsieh et al., 2005; Hsieh et al., 2009; Kim et al., 2009; Xue et al., 2009; He et al., 2011; Srinivasan et al., 2011; Jokinen et al., 2013). Hybrid substrates are defined as those produced using two or more of the other base materials shown in Figure 2.3. Examples of such combined materials include carbon fabrics, which are combination of non-metal and fibrous material (Hsieh et al., 2008a; Hsieh et al., 2008b; Hsieh et al., 2010), polybenzoxazine-modified glass (polymer and non-metal) (Wang et al., 2009), glass fiber (Meng et al., 2014), artificial surface using stainless steel and Polydimethylsiloxane (PDMS, a widely used silicon-

based organic polymer) (Guan et al., 2015 & Liu et al., 2016) and gold coated silicon substrate (Yadav et al., 2015).

Polymers are not too often used as base material for experimentation, with only four studies doing so, which are polydimethylsiloxane (PDMS) (Khosrani et al., 2005 & Zhang et al., 2016), polyethylene tereph-thalate (PET) (Tarrade et al., 2014) and hydrophobic segmented silicone-urea co-polymer (TPSC) (Soz et al., 2015). This could be due to their high costs.

Metal is clearly the most popular surface to be textured for super hydrophobicity as seen in Figure 2.3 with thirty-two publications focusing on this scope. Figure 2.4 tabulates the types of metal commonly used and it is evident that aluminium, copper and stainless steel are prominent metals. Since aluminium is widely used in many industrial fields because of their practical applications in anti-corrosion, fluid drag reduction and no-loss transportation (Yuan & Jin, 2010; Pan et al., 2010; Yao et al., 2010), it is a subject of great interest among researchers (Li et al., 2011; Liu et al., 2011; Shi et al., 2012; Yin et al., 2012; Ruan et al., 2013; Liang et al., 2014; Liu et al., 2015b; Long et al., 2015). The advantage of aluminium is that its oxide is chemically stable in air and this inertness avoids wettability transition between hydrophilicity and hydrophobicity caused by photo catalysis or oxidation–reduction reaction (Long et al., 2015).

Fabrication of functional superhydrophobic surfaces on aluminium alloy has an intense amount of industrial value and significance as it is structural engineering materials used in the fields of aerospace, automobile, building, and railway applications because of their excellent properties such as low density, excellent thermal and electrical conductivity, high specific strength and good cast ability.

Copper is a cost-effective engineering material, but exhibits poor corrosion resistance due to its high chemical action (Fan et al., 2014 & Ghelichkhah et al., 2015).

It is proposed that superhydrophobic film coating can adequately enhance the corrosion resistance because of block effect of air pockets in the film (Gao et al., 2014). Furthermore, corrosive droplets have the ability to easily roll off the superhydrophobic surface, which does not provide sufficient time to deteriorate the Cu substrate.

Hence, copper is the most popular material used to create super hydrophobic surfaces as seen in Figure2. 4. Many researchers, namely Guo et al., 2007; Liu et al., 2007; Chen et al., 2009; Song et al., 2009; Xi et al., 2009; Pan et al., 2010; Hashemzadeh et al., 2015; Liu et al., 2015a; Liu et al., 2015 d and Xiao et al., 2015 have reported their works on fabrication and optimization of parameters to achieve maximum super hydrophobicity on this substrate.

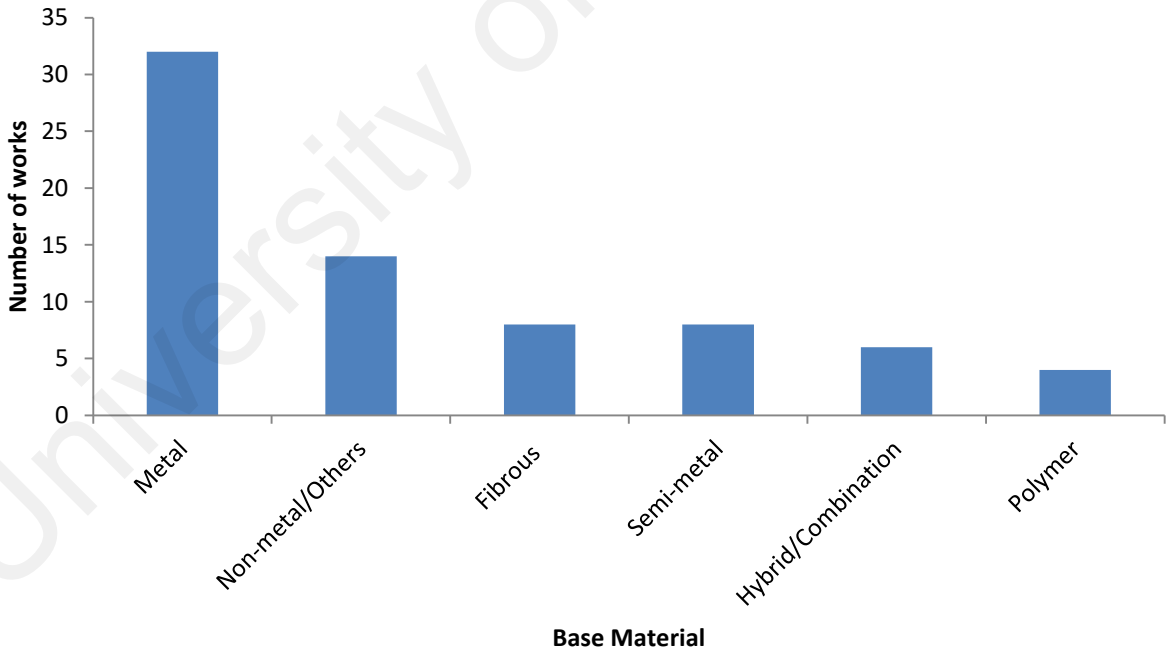

Figure 2.3: Various base materials used for superhydrophobic surface research

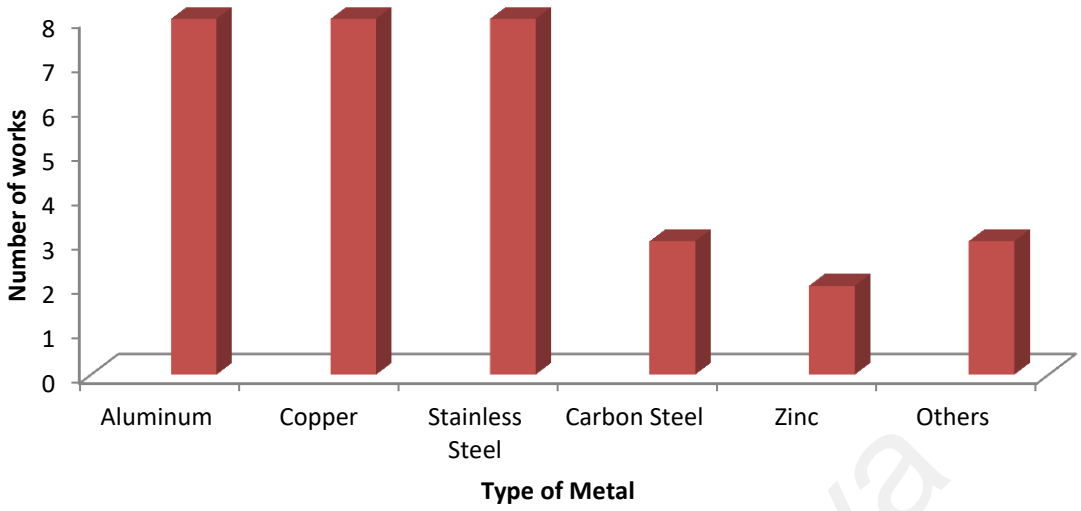

Figure 2.4: Types of metals used as base substrates

Stainless steel is another favorable material often used to create rough surfaces. Wang et al. (2007), Cui et al. (2009), Yang et al. (2010), Cho et al. (2015), Gong et al. (2015), and Escobar et al. (2016) have worked on this metal in recent years to establish knowledge in fabricating superhydrophobic stainless steel due to lack of studies on this metal compared to popular metals such as copper and aluminum.

Current researchers have shown an emerging interest on stainless steel as it is a common metal alloy used in industrial application and known for its good mechanical workability and anticorrosion properties (Li et al., 2014; Escobar et al., 2014). There were only three works reported on the usage of carbon steel plates, namely by Guo et al. (2012), Motlagh et al. (2013) and Chen et al. (2015), while two research groups tested the potential of zinc as a superhydrophobic substrate (YanLong et al., 2014 & Bayat et al., 2015).

Furthermore, there are some other materials experimented as base material. In particular, other metals that are investigated for their water repellency are tin-bronze (Hao et al., 2015), titanium (Cho et al., 2015), nickel, cadmium, gold and palladium

(Liu et al., 2015a). Research and analysis of newer materials apart from traditional substrates such as aluminum and copper has been reported in recent years as focus is now on the versatility of engineering materials in terms of application.

2.7 METHOD OF ROUGH SURFACE PREPARATION

A method to increase the hydrophobic properties of a surface is by enhancing its roughness. Hence, roughness-induced hydrophobicity has been a subject of intensive analysis. (Nosonovsky and Bhushan). Numerous studies have proposed that two-tiered/ multilevel roughness (produced by superposition of two or more roughness arrangement at different length scales) and fractal roughness could cause non-wettability (Herminghaus, 2000; Patankar, 2004; Sun et al., 2005). Likewise, scientific experimentation by Erbil et al. (2003) and Burton & Bhushan (2005) has demonstrated that roughness undeniably is the source of change in contact angle value.

Surface roughening is vital for the design of suitable surface structure because this supplies a capillary force that hinders liquid from infiltrating the grooves on the surface. (Aulin et al., 2009). Another study by Rabinovich et al. (2002) has established that an increasing effective radius of interacting particles will increase the capillary force. Consequently, liquid droplets will be able to diffuse easily into small gaps (< 2nm) on liquid-repellant surfaces.

Various methods have been applied for the construction of super-non-wetting surfaces such as wet chemical oxidation, electrodeposition, dip-coating, hydrothermal, spray deposition, chemical vapor deposition, sol-gel, grinding, sandblasting, particle coating, and etching (plasma, laser, chemical, electrochemical) (Valipour et al., 2014 and YanLong et al., 2014). These methods are shown according to the year in Figure 2.5.

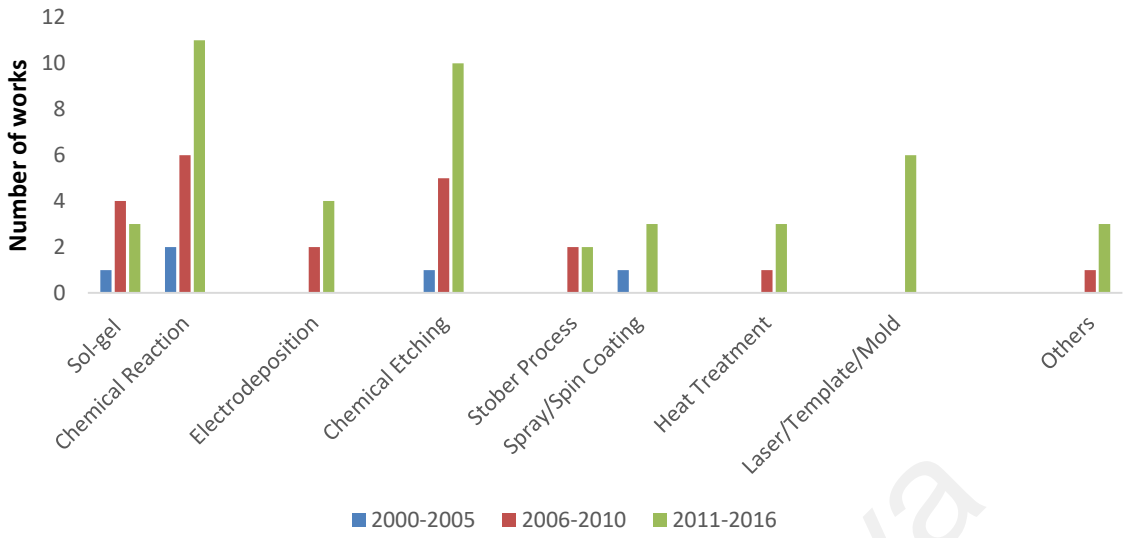

Figure 2.5: Methods of rough surface fabrication

During the pioneer years when this research scope was initiated (2000-2005), sol-gel (Nakajima et al., 2000) and chemical reactions were used to fabricate rough surfaces. Chemical reactions that were experimented are mixing nanoparticles with polymer (Hsieh et al., 2005), curing process (Khosrani et al., 2005), chemical etching, which is oxygen plasma etching (Shang et al., 2005) and spin-coating Li et al., 2005) only has one report each.

The second era of scientific analysis on liquid-repellant surfaces was from 2006-2010. This period saw the emerging application of processes such as sol-gel, chemical etching and chemical reactions. Generally, sol-gel coating method uses pre-prepared polystyrene spheres which are coated on substrates to create roughness (Liu et al., 2011). Sol-gel method was used to prepare silica nanoparticles (Yu et al., 2007; Hsieh et al., 2010; Yang et al., 2010) or the sol-gel matrix was dispersed in an acid-catalyzed sol of tetraethoxysilane (TEOS) and methyltriethoxysilane (MTEOS) (Lakshmi and Basu, 2009; Mahadik et al, 2010).

Chemical etching is also deduced to be a promising technology that gained popularity during the years 2006-2010. According to Hikita et al. (2009), many researchers have adopted this procedure as it relatively simple; do not involve any sophisticated experimental setup and prompts to produce hierarchical structures consisting of nano- and microscale properties. This surface is super-repellent to both oil and water.

The chemical reagents used for etching were nitric acid (Liu et al., 2007; Pan et al., 2010), hydrochloric acid (Nimittrkoolchai and Supothina, 2008), hydrofluoric acid (Saleema and Farzaneh, 2008), mixture of hydrofluoric acid and hydrogen peroxide (Kim et al., 2009). Meanwhile, the chemical reactions deployed are immersion (Guo et al., 2007; Wang et al., 2007), chemical wet-impregnation (Hsieh et al., 2008a), chemical vapor deposition (Hsieh et al., 2008b), alkali assisted surface oxidation (Chen et al., 2009), and replacement reaction (Song et al., 2009).

In the recent years in the development of non-wetting surfaces (2011-2016), applications of chemical reactions and chemical etching have been frequently reported in literature. Moreover, increasing trend of surface texturing using laser/template/mold, electrodeposition and spray/spin coating was observed. Chemical reaction used were anodization (Li et al., 2011), mixing reagents (Srinivasan et al., 2011; Das et al., 2012; Tian et al., 2015), catalytic chemical vapor deposition (Meng et al., 2014; Yadav et al., 2015), electrochemical micromachining (EMM) method (Hao et al., 2015), electrolytic process (Escobar et al., 2016).

Laser, template and mold technologies are relatively new which are steadily gaining immense popularity in this field. Picosecond laser was used by Gong et al. (2005) and they managed to achieve CA of 154.6 and SA of less than 5.5, which can be classified as super-non-wettability.

Additionally, Long et al. (2015) also used picosecond laser, attaining approximately the same CA of 154. Guan et al. (2015) fabricated biomimetic water bamboo leaves, which are liquid-repellant in nature by template transfer method using Polydimethylsiloxane (PDMS) replicas and obtained hydrophobic surface with CA=146.

The type of laser fabrication process which produced the highest contact is ultrafast laser ablation with CA of 164.5 and SA equivalent to 8.44. This study by Liu et al. in 2016 utilized PDMS negative replicas as substrates and created micro and nanoscale roughness on it. Latest work by Zhang et al. (2016) used PDMS to prepare gecko-inspired adhesive surfaces using micro-mold casting and reached CA of 155.

The morphology of a base material can be altered by the electrodeposition technique as well. Electrodeposition was performed using various electrolytes, namely copper sulfate (YangLong et al., 2014), copper chloride (Liu et al., 2015d) and composite coatings (Chen et al., 2015; Escobar et al., 2016). In addition, spray or spin coating was also used by scientists to induce roughness on base materials (Das et al., 2012; Lathe and Rao, 2012; Wang et al., 2014; Soz et al., 2015).

Lastly, other prevailing approaches apart from traditional methods have been effectively tested and optimized to achieve maximum contact angle values. These processes are listed in Table 1 below and amongst the recent technologies discovered, heterogeneous nucleation and growth of nanoparticles, area selective deposition (ASD) and hydrothermal method are ideal for rough surface assembly.

Table 2.1: Other commonly used surface roughness preparation methods

Method of Roughness Preparation	Reference(s)	Contact Angle, CA	Sliding Angle, SA
Heterogeneous nucleation and growth of nanoparticles	Liu et al., 2011	169	4
Hydrothermal method	Fu et al., 2012	153	Droplet can easily roll-off
	Cho et al., 2015	160.4	5
	Liu et al., 2015c	153	4
Stöber method	Liang et al., 2014	154.9	-
Oxygen and CF_4 plasma treatment	Tarrade et al., 2014	157	-
Area Selective Deposition, ASD	Xiao et al., 2015	160	4

2.8 SURFACE MORPHOLOGY AND SHAPES

Various forms of surfaces found in nature such as butterfly's wings, insects legs, lotus leaves and water bamboo leaves display super hydrophobicity with the self-cleaning ability, as the repelled droplet collects dust molecules when it slides off the surface (Cong et al., 2004). These natural surfaces have similar traits which are hierarchical structures which are micro to nanometer in size. Most surface-structure techniques are aimed at lowering the explicit surface microstructure geometry (Kwon et al., 2009).

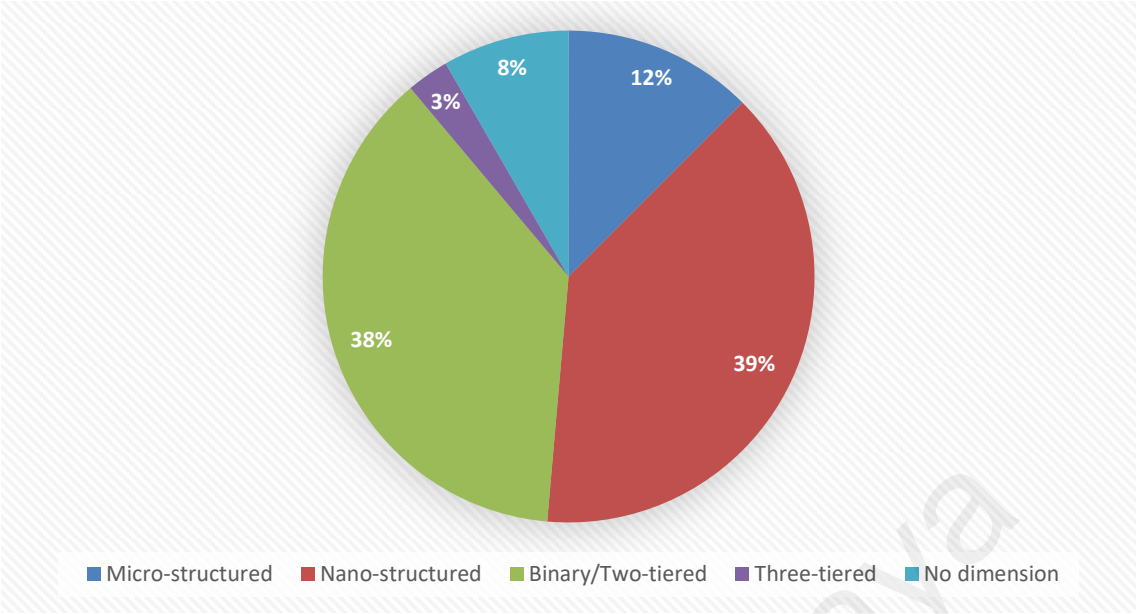

Figure 2.6: Surface morphology and microstructure

From Figure 2.6, it is seen that a collective amount of 77% of published journals managed to attain nano-structure (39%) and binary/two-tiered structure (38%, which is defined as containing micro and nanoscale structures). Based on review, the highest contact angle achieved till date is approximately 180º by the scientific investigation by Hao et al. (2015). They examined the dynamics of drop impact on single-tier micro textured surface (STMS), single-tier nanotextured surface (STNS) and two-tier hierarchical surfaces (HS) with micro-craters and ZnO nano-rods.

Comparison between the three types of morphology proves that the two-tiered hierarchical surface is optimum for non-wettability because HS with feature size of 40 µm/80 nm had CA value of 180º and sliding angle lesser than 1º. STNS (feature size = 80 nm) and STMS (feature size = 40 µm) recorded CA values of 165.8º and 132.1º respectively.

For HS, even when the droplet penetrated into the micro-concaves, there are plenty of ZnO nano-rods and micro-flowers spreading all over the side and bottom walls. Furthermore, the two-tiered arrangement further stabilizes the super hydrophobic

state by surging the energy difference between the Cassie and the Wenzel states. The stability of Cassie state at the nanostructure scale also allows the higher level structures to restore super hydrophobicity easily after the impact of a rainfall (Su et al., 2010).

In 2016, research by Escobar et al. accomplished contact angle of 175º and a very low sliding of 3.5º under 30 seconds electrolysis time. The surface morphology was hierarchical micro-nano structures which were textured with 2 μm pillars and scanning electron microscopy (SEM) revealed surfaces of the pillars were covered by nanoscale granular protrusions and grooves. The capability of hierarchical micro–nano structures' grooves to trap a fraction of the air facilitates the hydrophobicity of the material.

A small number of researchers have fabricated three-tiered composite structures that exhibit relatively excellent superhydrophobicity, reaching a contact angle value up to 170º and roll-off angle less than 5º (Hsieh et al., 2010 & Motlagh et al., 2013). The former states the three-tiered surface comprised of micro, sub-micro and nanoscale structures. The submicron-scale SiO_2 spheres and nanoscale CNTs attached to microscale CFs induced the secondary and tertiary surface topology, respectively.

The surface also doesn't need any further surface treatment to display enhanced water repellency and exceptional superhydrophobic stability. Previously, the authors (Hsieh et al., 2008b) created carbon fabrics (CFs) with micro/nanoscale two-tier roughness and had only achieved CA value of 169.7±2.2° despite undergoing surface treatment with perfluoroalkyl methacrylic copolymer.

Table 2.2 lists the papers published that involve micro-level surface texturing. It can be concluded that merely the surface morphology, whether it is micro, nano-scale or binary structured is not the sole determining factor for attaining excellent super-liquid-repellant surfaces. This is due to the fact that another crucial element also determines

this property, which is chemical composition and surface energy. Some studies show that although the surface merely has microstructures, it has high non-wettability due to an efficient surface treatment that lowers the surface energy (Mahadik et al., 2010; Srinivasan et al., 2011; Yin et al., 2011; Das et al., 2012; Lathe & Rao, 2012).

Table 2.2: Papers with micro-level surface morphology

Reference	Contact Angle (CA)	Sliding Angle (SA)
Yoon et al. (2009)	153º	4º
Mahadik et al. (2010)	172º	2º
Li et al. (2011)	152º	-
Srinivasan et al. (2011)	160º	2º
Yin et al. (2011)	161.2º	< 8º
Das et al. (2012)	158.5º	4º
Lathe & Rao (2012)	162º	6º
Guan et al. (2015)	146º	-
Zhang et al. (2016)	155º	7º

2.9 LOW SURFACE ENERGY COATING MATERIALS

Desired wettability is attained only when the chemical composition of their material has reached a low surface energy value. To achieve the super-non-wettable state, the surface free energy of the solid substrates shall be lesser than one quarter of that of the liquid, hence only is about a few mN/m. Reports state that the minimum surface energy groups in monolayer films are of the following order, $–CH_2 > –CH_3 > –CF_2 > –CF_2H > –CF_3$ (Steele et al., 2009; Aulin et al., 2009; Lin et al., 2006).

Therefore, it is to be noted that polymers, particularly fluoropolymers are the most popular coating material used to lower a surface's energy because of their tremendous amount of $–CF_3$ and $–CF_2$ groups (Xu et al., 2012). A paper published by

Hirao et al. (2007) has mentioned other benefits of fluoropolymers which are it possess good chemical/thermal stability and low friction coefficient and plays a role in the construction of surface structure.

Figure 2.7: Low surface energy coating materials

In this review, 22 works reveal the usage of fluoropolymer as surface coating substrate, namely Nakajima et al. (2000), Hsieh et al. (2005), Shang et al. (2005), Li et al. (2005), Yu et al. (2007), Hsieh et al. (2008 b), Chen et al. (2009), Hsieh et al. (2009), Kim et al. (2009), Pan et al. (2010), Park et al. (2011), Srinivasan et al. (2011), Wang et al. (2011), Yin et al. (2011), Das et al. (2012), Guo et al. (2012), Lakshmi et al. (2012), Shi et al. (2012), Meng et al. (2014), Bayat et al. (2015), Gong et al. (2015), and Guan et al. (2015).

In addition, perfluoroalkyl chains, which usually have 4-10 carbons, are able to multiply faster than others. This will result in greater ultimate thicknesses compared to shorter chain fluoropolymers. An extended fluorocarbon chain length will reduce the film's critical surface tension, thus improving CA outcome. The common type of

perfluoroalkyl chain used was perfluoroalkyl methacrylic copolymer, in three of the papers reviewed.

Silanes and/or silicates are other forms of polymers widely used in surface coating application. Research that applied this type of surface coating are Nakajima et al. (2000), Li et al. (2005), Shang et al. (2005), Nimittrkoolchai and Supothina (2008), Chen at al. (2009), Kim et al. (2009), Xue et al. (2009), Mahadik et al. (2010), Pan et al. (2010), Berendjch et al. (2011), Park et al. (2011), Wang et al. (2011), Yin et al. (2011), Liang et al. (2014), Guan et al. (2015) and Charyangi et al. (2016).

The silane/silicate materials highly preferred were fluoroalkylsilane (FAS), chlorotrimethylsilane (CTMS), tridecafluoro-1,1,2,2-tetrahydrooctyldimethylchlorosilane (TFCS), semifluorinated silane, 1H,1H,2H,2H-perfluorodecyltriethoxysilane, (tridecafluoro-1,1,2,2-tetrahydrooctyl)-tri- chlorosilane (FOTCS), Vinyltriethoxylsilane (VTEOS), trimethylchlorosilane (TMCS), Perfluorodecyltriethoxysilane (FDTES), alkylsilane agent, hexadecyltrimethoxysilane (HDTMS), 1H, 1H, 2H, 2H- perfluoroalkyltriethoxysilanes (POTS), fluorosilane, tetraethylorthosilicate (TEOS) and vinyltriethoxysilane (VTES), triethoxyoctyl silane (OTES) and hybrid mixtures of HDTMS/OTES.

Two other chemicals were also experimented in recent years as film materials, which are alcohol and acid. According to Li et al. (2011), alcohol coating was proven to provide a wettability transition from hydrophobicity to super-hydrophobicity as a self-assembled monolayer of octadecanethiol (ODT) significantly increased the CA from 96º to 152º. Modification with ODT subsides the surface energy which was favorable for increasing the water contact angle of the as-anodized bionic samples.

Besides that, journal written by YanLong et al. in 2014 also presented switchable wettability from superhydrophilicity to superhydrophobicity by altering the

surface chemical composition using dodecanethiol (DDT). This is a simpler and more versatile method compared to previous ones such as annealing and plasma treatment. After immersion in DDT, the surface hierarchical "flower pits" have trapped air in it, enabling it to be in the Cassie state that is conducive for superhydrophobicity. Studies by Liu et al. (2007) also show similar trends using ethanol.

A significant amount of research has also been done on acid as a coating substrate through the process of passivation (Saleema & Farzaneh, 2008; Liu et al., 2011; Ruan et al., 2013; Liu et al., 2015d). All of the works used stearic acid (SA) for surface modification besides the third reference which opted for lauric acid. Saleema & Farzaneh (2008) reinforced that stearic acid is essential for low surface energy because the SA passivated ZnO nanotowers experience a decrease in CA once the thermal desorption of SA occurs at elevated temperatures (184°C).

Liu et al. (2011) also attributed its high CA (169º) and low sliding angle (~4º) to the minimum surface energy of the SA coating. Similarly, the modification of lauric acid on the aluminum surface swiftly impairs its affinity for water/ice, which is a desired characteristic for heat exchanger/air-conditioning application. Various other chemicals have been tested for surface treatments such as Tetrafluoromethane (Yoon et al., 2009), zinc hydroxide (Fu et al., 2012), nickel coatings prepared from ammonium chloride (Hashemzadeh et al., 2015), copper film produced by reaction between copper sulfate and sulfuric acid (Liu et al., 2015a), 1,4-dimethylbenzene bath (Tian et al., 2015), cobalt film using platinum net as the inert anodic electrode (Xiao et al., 2015), and gold film (Liu et al., 2016).

2.10 CONTACT ANGLE AND ROLL-OFF ANGLE ACHIEVED

Figure 2.8 displays the contact angle and sliding angle achieved by all the literature reviewed chronologically according to the range of years. In the initial years of study circa 2000-2005, only a few works managed to achieve the superhydrophobic contact angle range of above 150º. As more researches were done between years 2006-2010, with significant improvement in technologies used to fabricate surfaces which were water-repellant, CA within range of 160º-170º was accomplished.

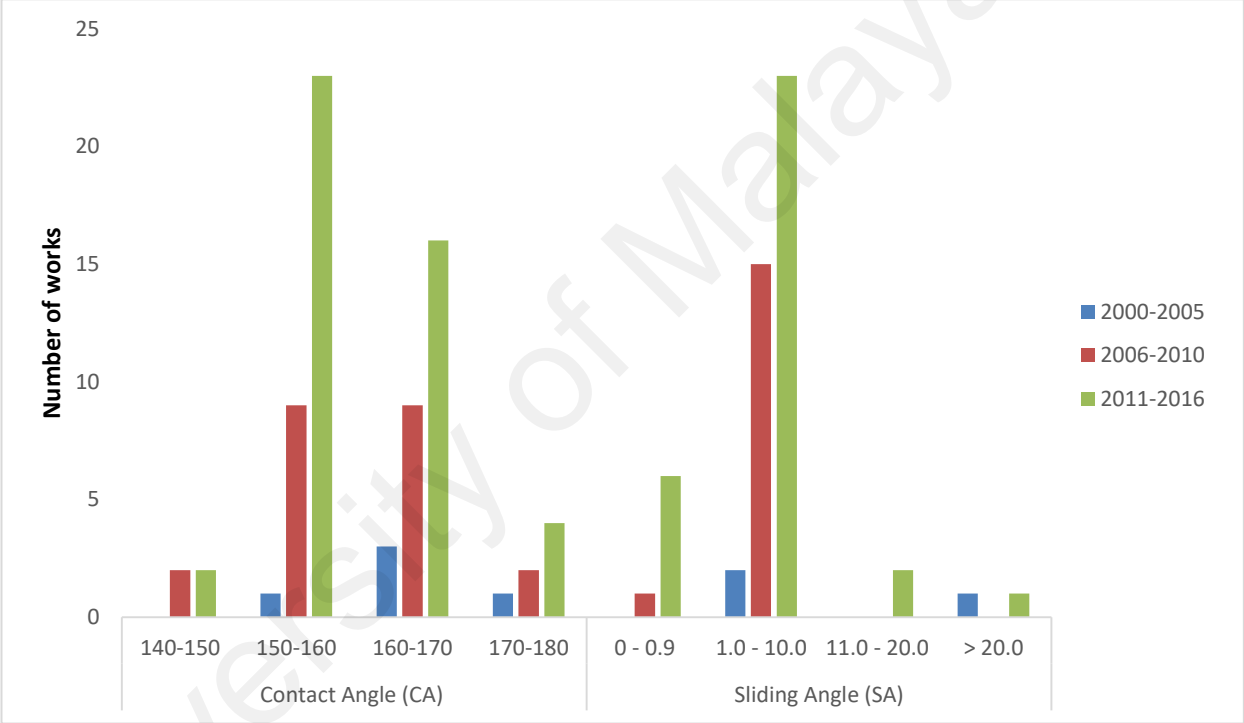

Figure 2.8: Water droplet mobility in terms of contact angle and sliding angle

This higher value of CA was even obtained on substrates other than commonly-used metal, such as carbon fabrics due to micro-and nano-scale protrusions constructed on the surface. Furthermore, scientific experimentation by Hsieh et al. (2009) was successful in recording contact angle of 168.4º and relatively low contact angle hysteresis of 2.1º using silicon substrates merely by surface alteration using perfluoroalkyl methacrylic copolymer without texturing the surface.

In recent years (2011-2016), a few researchers, have managed to reach CA between 170º and 180º and a study by Hao et al. in 2015 even displayed contact angle of 180º, which is classified as ultrahydrophobic (Extrand, 2002) and with a sliding angle less than 1º. In their paper, it was reported that surface roughness was created by etching micro-concaves via electrochemical micromachining (EMM) technique and fabricating nano-pillars of ZnO by a hydrothermal method without any further surface modification. This method was proven to be economical to be used on metallic planar surfaces and cylindrical inner surfaces.

Motlagh et al. (2013) used spray coating of silica sols to produce superamphiphobic coating with extremely high contact angle up to 170º and sliding angle of 1º. The surface energy was decreased by perfluorodecyltriethoxysilane. Moreover, Liu et al. (2015b) demonstrated that a one-step anodization process is feasible to create super-liquid repellant surfaces. Aluminum alloys were anodized in an electrolyte solution of myristic acid and aluminum nitrate, generating a coating with CA of 171.9º and SA of 6.2º.

Another electrochemical method was investigated by Escobar et al. (2016) where the surface was textured via an electrolytic process using nickel chloride and lauric acid in ethanol solution without any surface modification. This technique developed hierarchical micro-nano structures i.e. micro-pillars, which were covered by nanoscale granular protrusions and grooves. The resultant surface exhibited excellent superhydrophobicity with contact angle of 175º and roll-off angle equivalent to 3.5º. TOF-SIMS analysis revealed that superhydrophobic layer was formed due to the reaction between Ni^{2+} ions and lauric acid on the stainless steel surface.

2.11 DURABILITY OF SURFACE AND POTENTIAL APPLICATIONS

Despite intense research of superhydrophobic surfaces to be utilized as engineering materials, numerous challenges in its practical application still exists. The micro/nano-structure, if damaged, could lead to a swift decrease of superhydrophobicity. Although the topographical structure of a coating is not damaged, the degrading of the low surface energy layer could also affect its liquid-repellant feature (Zhang et al., 2013). Hence, various studies were conducted to improve the durability and mechanical robustness of super hydrophobic materials for commercial applications.

Research by Tian et al. (2015) reported that the CA of polycarbonate nixed with silver loaded modified montmorillonite (Ag-Mt/PC-1.5) reduced by 10% only after being subject to continuous water flow at rate of 0.2mL/s for a week, indicating good durability. Additionally, when observed under the naked eye, there were no signs of obvious contamination after the samples were kept outdoors, under temperatures of 15°C - 33°C, which implies that it is ideal for large-scale outdoor applications.

In 2015, Liu et al. synthesized copper zig-zag micro-strip coating, which after tested using the tape peeling method showed robust adhesive strength to its copper substrate. This result proves that the coating is a suitable candidate to be used for corrosion protection of copper or its alloys. Works by Charyungi et al. (2016) have reported that their superhydrophobic coatings were resilient as the treated fabrics were able to perform even after abundant ultrasonication treatment in an ethanol bath.

Bayat et al. (2015) investigated PTFE/ZnO nanorods thin films with UV-resilient superhydrophobicity and found that its highest CA of 158º remains unchanged under normal day light irradiation for up to six months. Samples tested with UV illumination for different periods of time also exhibited stable wettability behavior

which is due to the presence of PTFE coating. Another study by Yin et al. (2012) investigated the effect of environmental factors such as relative humidity and concluded that loss of non-wettability prompted by water condensation under high humidity and low temperature can be revived after condensed water evaporated.

Transparent silica coatings fabricated by Mahadik et al. (2010) displayed imperviousness against strong acids by not even allowing strong acids (100% concentration) to wet its surface besides retaining its superhydrophobicity up to a temperature of 550°C. Similarly, the thermal stability of water-repellant PTFE films was examined from room temperature to 430°C (Gong et al., 2015). Results verify that the micro-nano dual arrangement on PTFE films and its superhydrophobicity is thermally substantial up to 340°C, but it is lost above 370°C. The samples were kept in closed containers for several months to test its time durability and showed minimal change in its CA up to 120 days.

Apart from the conventional superhydrophobic surface applications of self-cleaning, anti-sticking, anti-icing, and anti-corrosion, it has a huge potential in the biomedical field, particularly for implants, breast prosthesis, shunt valve for hydrocephalus, and pace maker lead insulator (Khorasani et al., 2005). PDMS substrates possess adequate resistance to hydrolytic and enzymatic degradation in the body and are compatible with blood. Soft tissue substitutes are often made of silicon owing to its excellent softness, stability and bio-inertness (Sonoda et al., 2001).

Materials with micro and nano-scale roughness also are vital for microelectronic application. The waterproof nature of such substrates enables it to be used in catalysis, photonic crystals, gas sensors, optical-electronic devices (Li et al., 2005) and for electrical insulation, piezeoelectric and photovoltaic devices, photonics and microelectronic circuits (Saleema and Farzaneh, 2008).

Research by Das et al. (2012) produced conductive polymer composite films which could function as EMI shielding materials. In field effect transistor (FET) based capacitive sensors, the superhydrophobic surface results in the omission of surface discharge caused by the leakage current even at relatively high humidity. In solar cells, self-cleaning property minimizes the buildup of dirt and mineral residue that can block the sun light from the panels (Gwon et al., 2014 & Yadav et al., 2015).

Other miscellaneous uses of superhydrophobic substrates include large-scale ocean industrial applications (Liu et al., 2007), industrial separation of oil and water and environmental protection (Wang et al., 2007), bio-separation devices for liquid transportation without loss and microfluidic devices (Hsieh et al., 2008b). Controllable super-repellant surfaces developed by Kim et al. (2009) can be applied in water harvest, anti-biofouling, and as highly lubricated surfaces with extremely low friction.

CHAPTER 3

METHODOLOGY

3.1 OVERVIEW

This chapter describes the research methodology for this project. Research methodology is a systematic way to solve a problem. It is a science of studying how research is to be carried out and the procedures by which researchers go about their work of describing, explaining and predicting phenomena. The work plan of research, steps that were followed and materials needed for this project are discussed in this chapter.

Aluminum substrates were used for this project as it is a common material used in the engineering industry for various applications. The substrates went through pre-treatment in which they are cleaned in a sonicator using distilled water and acetone. The most favorable etching parameters/conditions required to achieve maximum contact angle when using a mixture of ethanol solution of hydrochloric acid and myristic acid as the etchant were investigated.

Subsequently, four experiments were conducted to investigate the effect of various etching time, myristic acid concentration, type of aluminum substrate and impact of reaction temperature on the resultant non-wetting characteristic of the product. Then, the samples were subject to post-treatment which consisted of rinsing to remove any acid residue and drying in an oven.

Next, the surface contact angle of the samples was measured to characterize its non-wetting property as either hydrophobic or superhydrophobic. Lastly, the final product after chemical treatment was examined with Scanning Electron Microscopy (SEM) to observe its surface topography and geometry of the micro-nano structures to

determine if a rough surface has been fabricated. Using Energy Dispersive Spectroscopy (EDS), the type of elements present on the as-produced surface was identified.

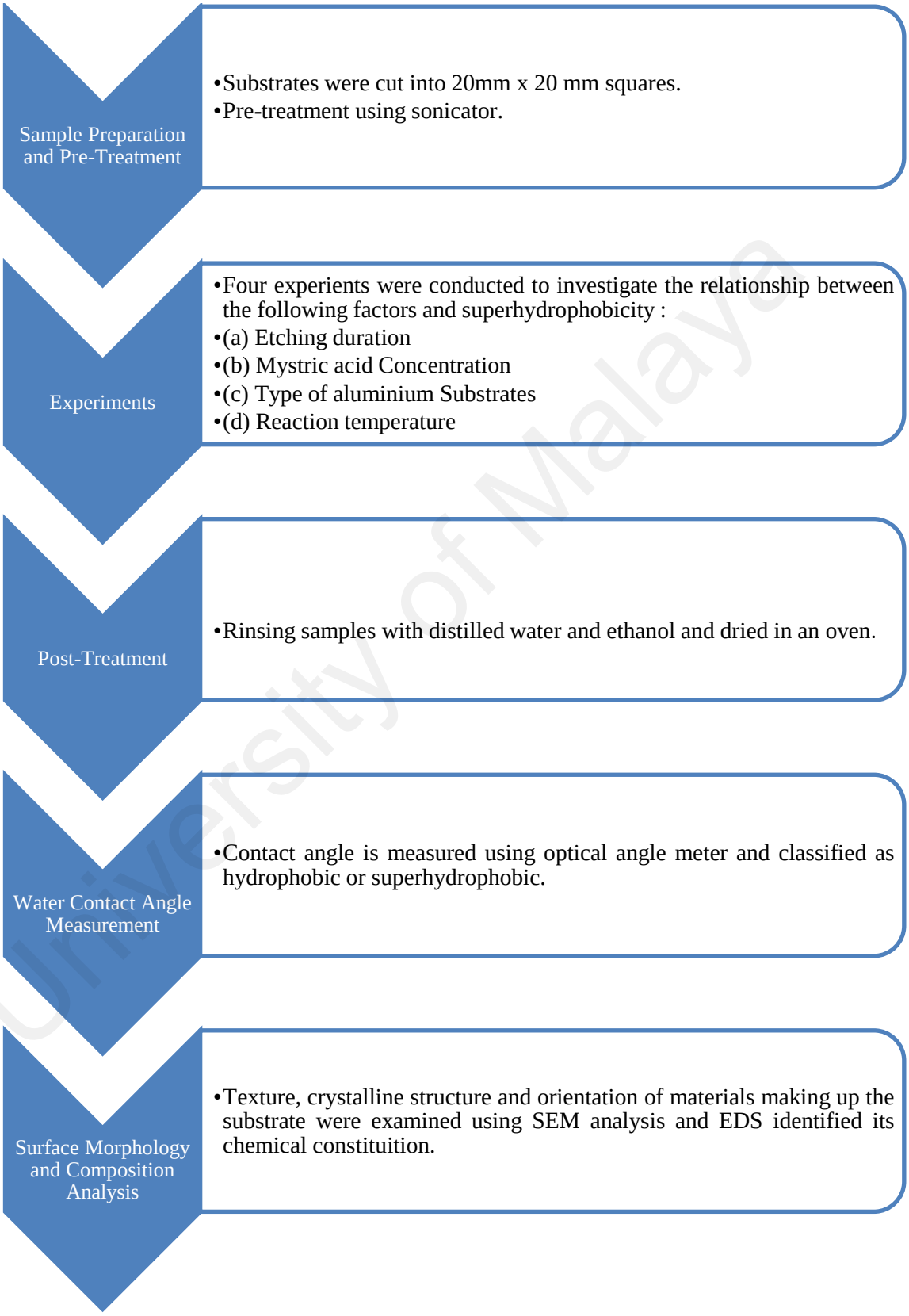

Figure 3.1: Summary of Experimental Procedures

3.2 MATERIALS

The substrates used for this research were aluminum alloy Al3102, in three different types which were the fin, foil and plate purchased from Logamweld (M) Sdn Bhd in Petaling Jaya. The thickness of the fin, foil and plate were 0.1 mm, 0.2 mm and 1.5 mm respectively as shown in Figures 3.2, 3.3 and 3.4. All substrates were cut into plates according to the size 20 mm x 20 mm. Hydrochloric acid (HCl), ethanol, acetone and distilled water were purchased from JS Galaxy Enterprise, Kuala Lumpur. HCl and ethanol were obtained in molarities of 1 mol/l. Myristic acid [$CH_3(CH_2)_{12}COOH$] was procured from R&M, UK in powder form (bottle).

Figure 3.2: Aluminum fin sample of thickness 0.1 mm

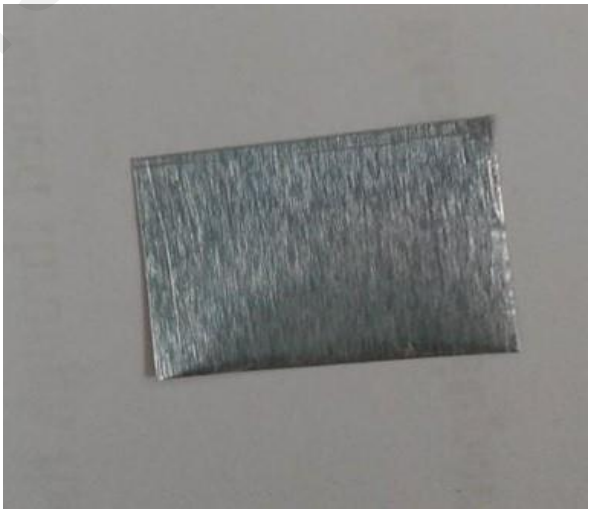

Figure 3.3: Aluminum foil with thickness of 0.2 mm

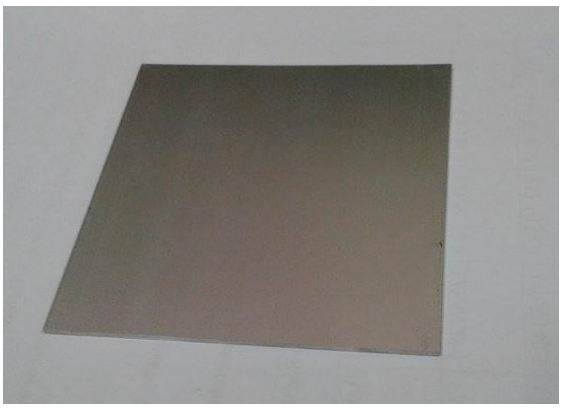

Figure 3.4: Aluminum plate with thickness of 1.5 mm

3.3 SAMPLE PREPARATION AND EXPERIMENTATION

Preliminarily, all the commercial aluminum plates were wiped with ethanol to remove existing residue and dust from the surface. Then, the surface was cleaned ultrasonically with acetone and distilled water in a sonicator for 20 minutes and allowed to dry for half an hour. Next, the plates were used for different experiments according to the procedures described in the following subsection adapted by the works of Pan et al. (2010), Zhang et al. (2011), Ruan et al. (2013) and Liu et al. (2015).

3.3.1 Effect of Different Etching Duration on Superhydrophobicity

Three pre-cleaned aluminium fins (thickness =0.1mm) labelled A, B and C were immersed in ethanol solution of hydrochloric acid and myristic acid and heated. Sample A, B and C was etched for 10 mins, 15 mins and 20 mins respectively. All other parameters such as ethanol volume (25ml), HCl quantity (5g/l), myristic acid quantity (3 g/l), and reaction temperature (70 °C) were fixed. The volume of HCl and myristic acid used was 200 ml for all four experiments.

3.3.2 Effect of Myristic Acid Concentration on Superhydrophobicity

The prepared aluminium foil (Samples D, E and F) were etched for 15 mins with a heated solution of 5g/l HCl dissolved in 25ml ethanol with manipulation of the

myristic acid concentration. Hence, sample D was etched using 1 g/l of myristic acid mixed into the ethanol solution of HCl, while sample E used 2 g/l of myristic acid and sample F used 3 g/l of myristic acid. Samples D, E and F were subject to a reaction temperature of 70 °C.

3.3.3 Effect of Type of Aluminium Substrates on Superhydrophobicity

In experiment 3, comparison between aluminium fin (sample G), foil (sample H) and plate (sample I) was done. The thickness of sample G, H and I were 0.1mm, 0.2 mm and 1.5 mm respectively. The etching period was constant for all samples at 15 minutes and ethanol volume was 25 ml. The quantity of hydrochloric acid used was 5g/l and 3 g/l of myristic acid was used. Samples G, H and I were immersed into the solution at 70 °C for 15 minutes.

3.3.4 Influence of Reaction Temperature on Superhydrophobicity

To investigate the relationship between temperature of etchant reaction (reaction between aluminium substrate and etchant chemicals) and the resultant contact angle, aluminium fin samples were tested under the temperatures of 50°C, 55°C, 60°C, 65°C, 70°C, 75°C and 80°C. The etchant mixture was heated using a laboratory heater until these desired temperatures were achieved, then samples dipped into these mixtures were labelled as J, K, L, M, N, O, P respectively.

Other parameters are as the following: etching period was 15 minutes, 25 ml of ethanol was used, 5g of HCl and 3 g/l of myristic acid as the etchant. After these experiments, the substrates went through post-treatment by rinsing with distilled water and ethanol to discard any acid residue and dried in an oven at 80°C for 30 minutes.

Post-treatment for all samples A – P was under these fixed conditions to ensure consistency in terms of results. The simulation cases for all 4 experiments were tabulated in Table 3.1 to show which parameters were manipulated and kept constant for each case. Steps taken during experimental procedures are shown in Figures 3.5 and 3.6.

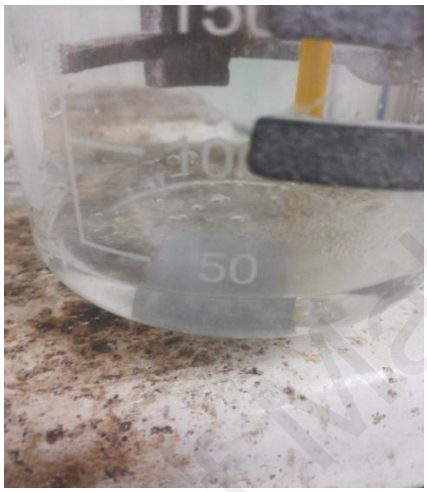

Figure 3.5: Aluminium foil immersed into etchant solution

Figure 3.6: Experimental set-up to heat etchant and substrate using laboratory heater

Table 3.1: Simulation cases of parameters for experiments 1-4

Experiment	Etching Duration (mins)	Ethanol Volume (ml)	HCl (g/l)	Myristic Acid (g/l)	Substrate Type	Al thickness (mm)	Temperature (˚C)	Contact Angle (º)
1	10	25 (Constant)	5 (Constant)	3 (Constant)	Fin (Constant)	0.1 (Constant)	70 (Constant)	145.6±1.3
	15							**159.4±1.1**
	20							157.8±0.5
2	15 (Constant)	25 (Constant)	5 (Constant)	1	Fin (Constant)	0.1 (Constant)	70 (Constant)	140.3±1.6
				2				150.5±1.0
				3				**156.9±1.5**
3	15 (Constant)	25 (Constant)	5 (Constant)	3 (Constant)	**Fin**	**0.1**	70 (Constant)	**159.3±1.0**
					Foil	0.2		155.2±1.3
					Plate	1.5		150.4±1.6
4	15 (Constant)	25 (Constant)	5 (Constant)	3 (Constant)	Fin (Constant)	0.1 (Constant)	50	116.9±2.8
							55	120.8±6.5
							60	135.7±2.1
							65	139.2±2.1
							70	**152.2±2.0**
							75	142.2±1.1
							80	132.2±1.3

3.4 WETTABILITY MEASUREMENTS, SURFACE COMPOSITION AND MORPHOLOGY ANALYSIS

3.4.1 Wettability Measurements

Post experiments, the surface contact angle of the samples possessed a definite contact angle value, which characterizes its non-wetting property. The contact angle was measured using an optical angle meter shown in Figure 3.7 (OCA 15EC, Dataphysics instruments GmbH, Germany) equipped with SCA20 image analysis software to compute the static contact angle (CA) of the droplet (Hao et al., 2015). The volume of the water droplet used was 5μL at dispensing rate of 1 μL/s. The approach used for dispensing was the static sessile drop method. Five measurements of CA were taken for each sample and the average value was taken.

A sessile droplet was placed on the horizontal surface and it was tilted until the droplet begins to slide. The angle subtended at the front of the droplet is the advancing contact angle (θ_{adv}), whereas that at the rear is the receding contact angle (θ_{rec}). The sliding behaviour of the droplet on the inclined superhydrophobic surface was observed directly by recording dynamic images using a high-speed digital camera system mounted on the contact angle meter and the advancing contact angle and the receding contact angle were measured from these pictures. The contact angle hysteresis is the difference between the advancing and receding angles, given by the expression CAH = $\theta_{adv} - \theta_{rec}$.

3.4.2 Surface Morphology and Composition Analysis

Scanning electron microscopy (SEM) images and Energy Dispersive Spectrometer (EDS) analysis were taken by Hitachi SU8220 field-emission scanning electron microscopy (FE-SEM) machine in the Department of Chemistry, Faculty of Science, University Malaya. The machine is shown in Figure 3.8.

The scanning electron microscope (SEM) uses a focused beam of high-energy electrons to generate a variety of signals at the surface of solid samples. The signals that are produced from electron-sample interactions reveal data about the sample in terms of external morphology (texture), chemical composition, and crystalline structure and orientation of materials making up the sample.

Energy Dispersive Spectroscopy (EDS) is used in conjunction with SEM and is a type of chemical microanalysis to obtain the surface composition. In this analysis, the x-rays emitted from the sample during bombardment by an electron beam are detected to characterize the elemental composition of the analysed volume. Features or phases as small as 1 µm or less can be analysed.

Figure 3.7: OCA 15EC optical angle meter to measure water contact angle

Figure 3.8: Hitachi model SU8220 field-emission scanning electron microscopy (FE-SEM) with EDS

CHAPTER 4

RESULTS AND DISCUSSION

4.1 OVERVIEW

The results of various experiments conducted to check the effect of different etching duration, myristic acid concentration, type of aluminium substrate (in terms of thickness) and reaction temperature on superhydrophobicity is presented in this chapter. Superhydrophobicity was determined using the contact angle values obtained through the optical angle meter equipped with SCA20 image analysis software. Post-analysis on the surface morphology and chemical composition was done by SEM and EDS respectively.

4.2 EFFECT OF DIFFERENT ETCHING DURATION ON SUPERHYDROPHOBICITY

Table 4.1 shows the results of experiment 1 to determine the effect of different etching duration on superhydrophobicity. Figure 4.1 and Table 4.1 shows the water CA datum for aluminium foil etched at durations of 10 mins, 15 mins and 20 mins. The resultants CA are 145.6º±1.3º, 159.4º±1.1º and 157.8º±0.5º respectively. It is noticeable that the contact angle increases to a peak and then decreases with the extended etching duration. The maximum CA is 159.4º at etching duration of 15 minutes. Hence, the optimum etching duration is concluded to be 15 minutes.

Table 4.1: Contact angle values for various etching durations

Sample	Etching Time (mins)	Ethanol Volume (ml)	HCl (g/l)	Myristic Acid (g/l)	Al Substrate Type	Al Thickness (mm)	Reaction Temperature (°C)	Contact Angle (°)
A	10	25	5	3	Fin	0.1	70	145.6±1.3
B	15	25	5	3	Fin	0.1	70	159.4±1.1
C	20	25	5	3	Fin	0.1	70	157.8±0.5

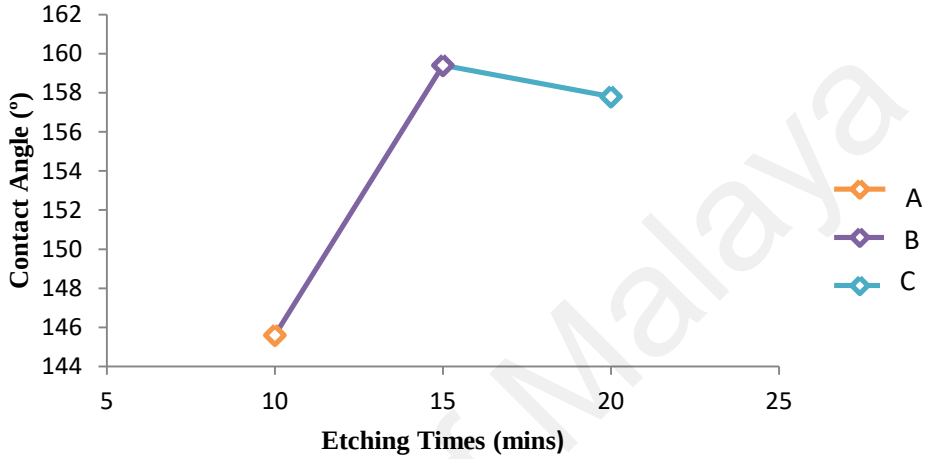

Figure 4.1: Effect of etching duration on water contact angle

Air trapped on the solid surface is essential for superhydrophobicity due to the fact that the water CA of air is approximately 180º (Jiang et al., 2004). Few cavities are present in the surface etched for 10 minutes, and labyrinth structures which can trap air through the dispersed protuberances of asperities have developed. This phenomenon enables the droplet to be practically resting on a layer of air (Hosono et al., 2005).

Nonetheless, a large equilibrium CA is only attained when small solid fraction thin pillars and dual scaled textures are present concurrently (Li and Amirfazli, 2007). At etching duration of 15 minutes, the largest CA was obtained because nano-protrusions have appeared on the micro protrusions to achieve rough dual labyrinth structures with finer pillars as seen in Figure 4.3.

However, when the etching duration was increased to 20 minutes (Figure 4.4), there is a slight decline in CA value. This is because the macrostructure asperities on the surface are damaged to an extent, enlarging the cavities which reduce the contact angle. It is predicted if the etching duration is further increased; the CA will exhibit a declining trend up to a point where thereafter the value stabilises. This hypothesis is supported by the research of Ruan et al. (2012) and Zhang et al. (2010) which recorded similar results.

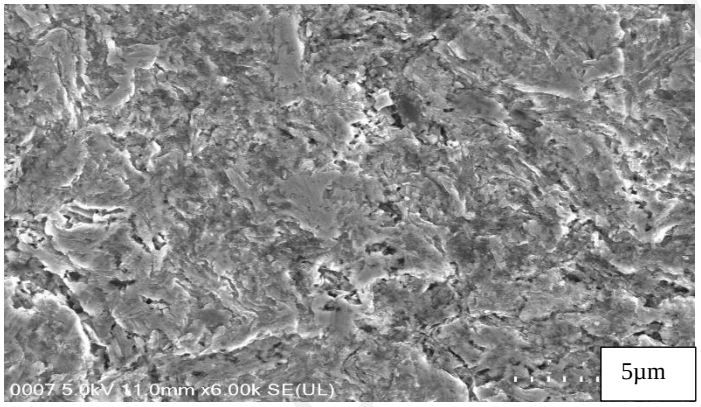

Figure 4.2: SEM image of sample etched for 10 minutes producing CA = 145.6±1.3º

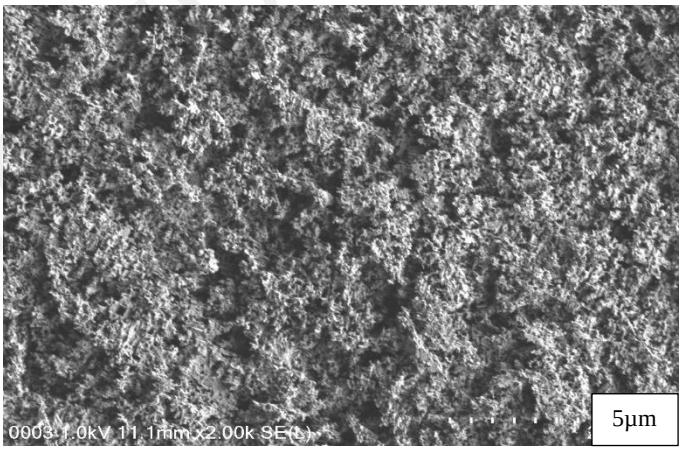

Figure 4.3: SEM image of sample etched for 15 minutes producing CA = 159.4±1.1º

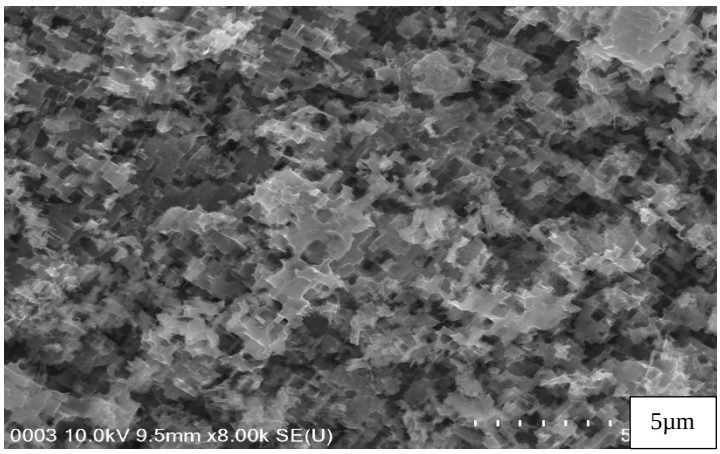

Figure 4.4: SEM image of sample etched for 20 minutes producing CA = 157.8±0.5º

4.3 INFLUENCE OF MYRISTIC ACID (MYA) CONCENTRATION ON SUPERHYDROPHOBICITY

Few studies namely by Jennings et al. (1998) and Jennings et al. (2003) reveal that thick coating films from long-chain fatty acids provide immense protection to the basal metal surface compared to thinner films, from both performance and lifetime aspects. Hence, there is a need to investigate the ideal myristic acid concentration for maximum superhydrophobicity. Table 4.2 and Figure 4.5 display the contact angles obtained when different concentration of myristic acid (MYA) was used during the chemical etching process.

Table 4.2: Contact angle values for different myristic acid concentrations

Sample	Etching Duration (mins)	Ethanol Volume (ml)	HCl (g/l)	Myristic Acid (g/l)	Al Substrate Type	Al Thickness (mm)	Reaction Temperature (°C)	Contact Angle (°)
D	15	25	5	1	Fin	0.1	70	140.3±1.6
E	15	25	5	2	Fin	0.1	70	150.5±1.0
F	15	25	5	3	Fin	0.1	70	156.9±1.5

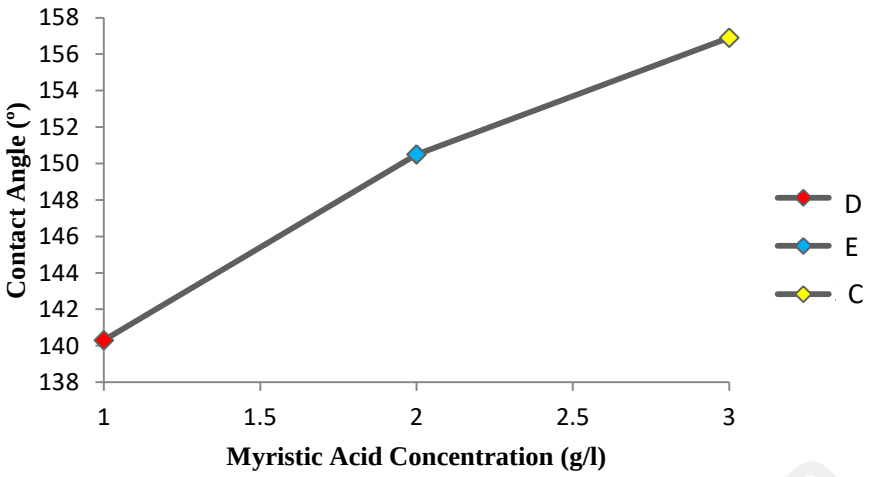

Figure 4.5: Effect of myristic acid concentration on water contact angle

The myristic acid concentration has prominent influence on the wettability of the aluminium foil surface. It is observed that water CA gradually increases with higher concentration of myristic acid. The results indicate that the grafted myristic acid chains is inadequate when the MYA concentration used is 1 g/l or lesser, while the grafted MYA chains increased at concentration of 2 g/l, just attaining superhydrophobic state (CA = 150.5º±1.0º). The CA reached maximum value of 156.9º±1.5º when the MYA concentration is 3 g/l.

At higher concentrations of the reactant, structures such as micro-rods and raised microplates are formed on the surface. As a result, porous structure density of the solid aluminium foil is stepped-up. Coatings made from higher concentration of MYA produce more uniform surfaces, thus superhydrophobic film can be formed compactly. These results demonstrate that the wettability of Al foil can switch from hydrophobic to superhydrophobic by controlling surface morphology merely by adjusting the etchant/low-surface energy agent concentration.

The results obtained from this experiment are similar to studies by several other researchers whom investigated the effect of fatty acid concentration on surface

morphology and superhydrophobicity. Research by Rezayi & Entezari (2016) demonstrated that water contact angle steadily rises with fatty acid concentration upsurge. The maximum CA achieved is 156.16º ± 2.89º at stearic acid concentration of 0.021M as seen from Figure 4.6, before remaining constant at the subsequent concentration of 0.030M.

Wang et al. (2012) also verified these findings and inferred that enhanced wettability is fabricated at higher fatty acid concentrations because the diameter of pores produced due to etching on the surface are significantly larger. Larger size pores allow greater volume of air to be trapped in it, consequently increasing f_a, which is the area ratio of air that contacts the solid surface. High percentage of f_a (f_a >90%) is crucial for the fabricated surface to exhibit water-repellence characteristic (Park et al., 2011).

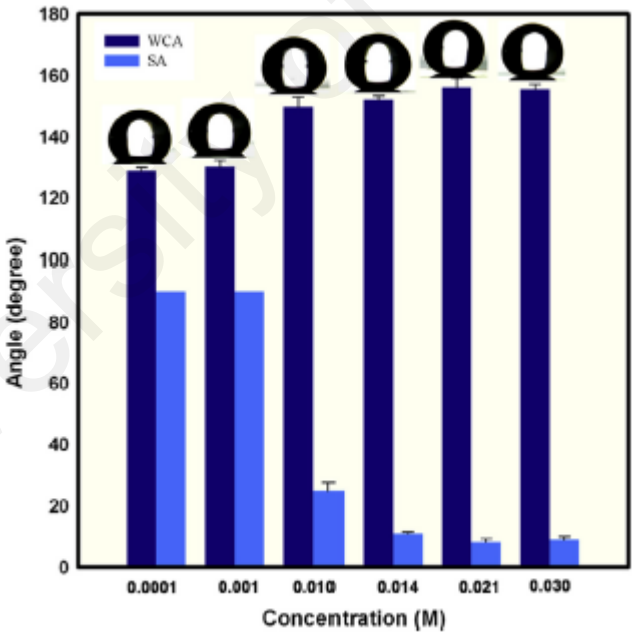

Figure 4.6: Contact angle and sliding angle versus different concentrations of stearic acid (STA) adapted from Rezayi & Entezari (2016)

4.4 INFLUENCE OF DIFFERENT TYPES OF ALUMINIUM SUBSTRATE ON SUPERHYDROPHOBICITY

For this project, three types of aluminium substrate were tested to observe which state of wetting is achieved and to determine which is the most favourable for superhydrophobicity. The specimens used are aluminium fin grade Al3102 (t=0.1mm), foil (t=0.2mm) and plate (t=1.5mm). From the results tabulated in Table 4.3 and Figure 4.7, it is noted that all three samples have attained the superhydrophobic state, with the highest CA of 159.3º±1.0º produced on the thinnest surface which is the foil.

Thin films/layer have been proved to be conducive to obtain CA values above 150° by the works of other scientists such as Zhang et al. (2016), Thieme et al. (2013) and Li et al. (2007). The justification for this inference is that thinner films contain more porous structures, which allows easier surface modification by the low-surface energy reagent, which in this case is myristic acid. In 2006, Pacifico et al. have established that thinner film layers produce CA as high as 161.3º and microsphere size also is a factor for surface roughness, with smaller sphere size causing a steady increase in CA.

Table 4.3: Contact angle values for different types of aluminium substrate

Sample	Etching Duration (mins)	Ethanol Volume (ml)	HCl (g/l)	Myristic Acid (g/l)	Al Substrate Type	Al Thickness (mm)	Reaction Temperature (°C)	Contact Angle (°)
G	15	25	5	3	Fin	0.1	70	159.3±1.0
H	15	25	5	3	Foil	0.2	70	155.2±1.3
I	15	25	5	3	Plate	1.5	70	150.4±1.6

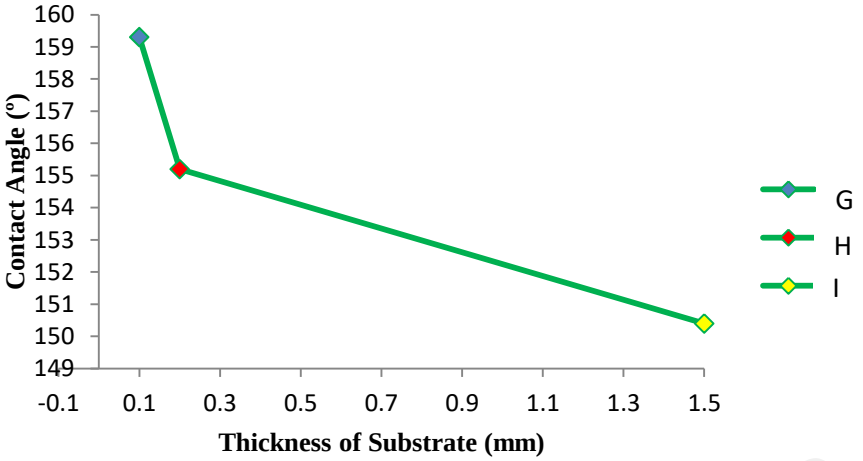

Figure 4.7: Effect of type of aluminium substrate in terms of thickness on water contact angle

Table 4.4: Contact angles measured on silver surfaces patterned with 5.5µm microspheres using NSL covered with SAM of 1H,1H,2H,2H-Perfluorodecanethiol adapted from Pacifico et al. (2006)

Film thickness (nm)	CA of bare silver (º)	CA with 1H,1H,2H,2H-Perfluorodecanethiol (º)
10	62.8	106.5
20	63.6	118.2
40	67.5	147.0
80	66.0	161.3

4.5 EFFECT OF VARIOUS REACTION TEMPERATURES ON SUPERHYDROPHOBICITY

According to Xu et al. (2007), the wetting transition from a hydrophobic surface, which is in the Wenzel state and a superhydrophobic surface which is in the Cassie-Baxter state occurs at a certain reaction temperature. This particular temperature varies between materials and the effect of surface morphologies fabricated at various etching temperature on the wetting behaviour of aluminium fin was also investigated in this project.

Table 4.5 shows the CA values observed at temperatures in the range of 50°C to 80 °C. It is seen from Figure 4.8 that the CA values increase steadily from 116.9° at 50°C, reaching a maximum value of 152.2º at 70°C, and thereafter declining at elevated temperatures up to 132.2º±1.3º. Hypothetically, it seems as temperature is altered, the surface morphology undergoes significant changes that influence the resultant CA (Song et al., 2009).

Table 4.5: Contact angle values for samples subject to different reaction temperatures

Sample	Etching Time (mins)	Ethanol Volume (ml)	HCl (g/l)	Myristic Acid (g/l)	Al Substrate Type	Al Thickness (mm)	Reaction Temperature (°C)	Contact Angle (°)
J	15	25	5	3	Fin	0.1	50	116.9±2.8
K	15	25	5	3	Fin	0.1	55	120.8±6.5
L	15	25	5	3	Fin	0.1	60	135.7±2.1
M	15	25	5	3	Fin	0.1	65	139.2±2.1
N	15	25	5	3	Fin	0.1	70	152.2±2.0
O	15	25	5	3	Fin	0.1	75	142.2±1.1
P	15	25	5	3	Fin	0.1	80	132.2±1.3

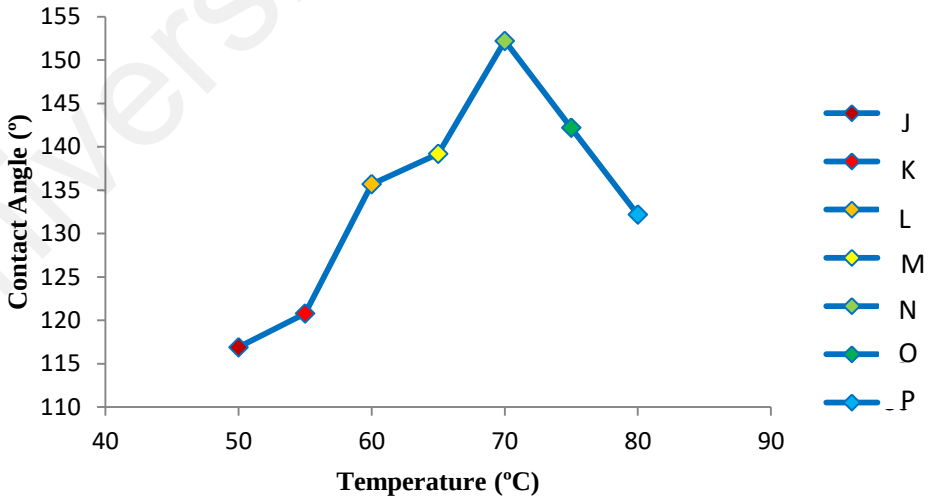

Figure 4.8: Effect of temperature on water contact angle

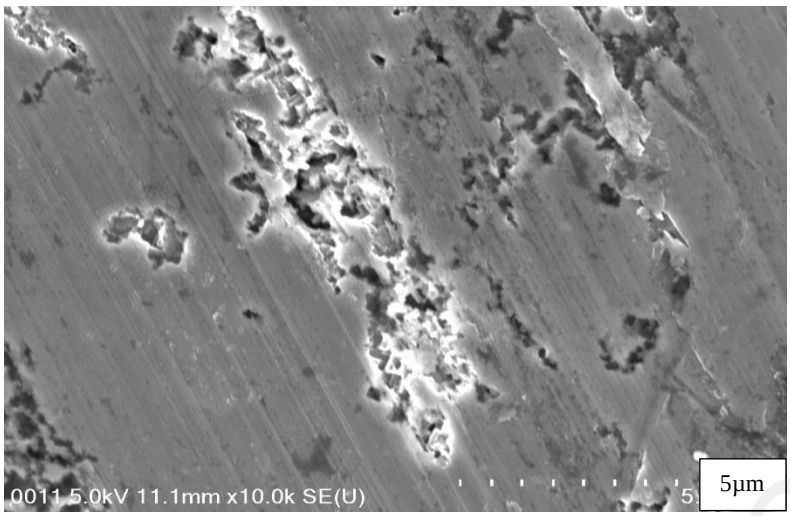

Figure 4.9: Sample J etched subject to reaction temperature of 50°C

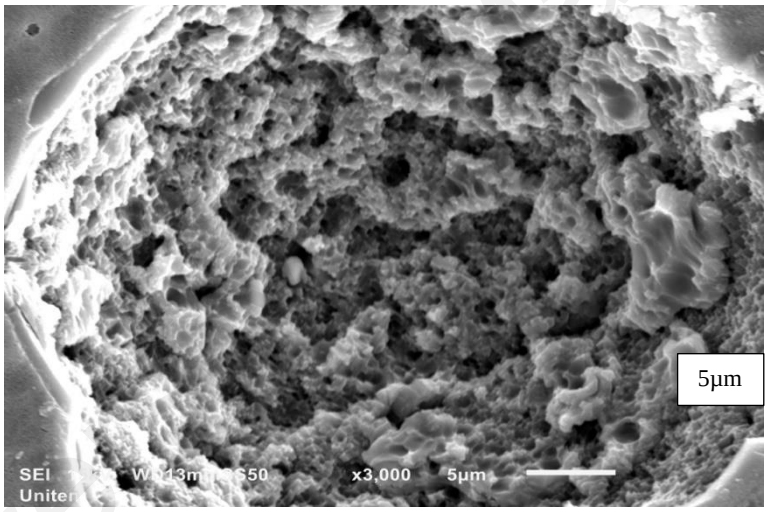

Figure 4.10: Sample N etched subject to reaction temperature of 70°C

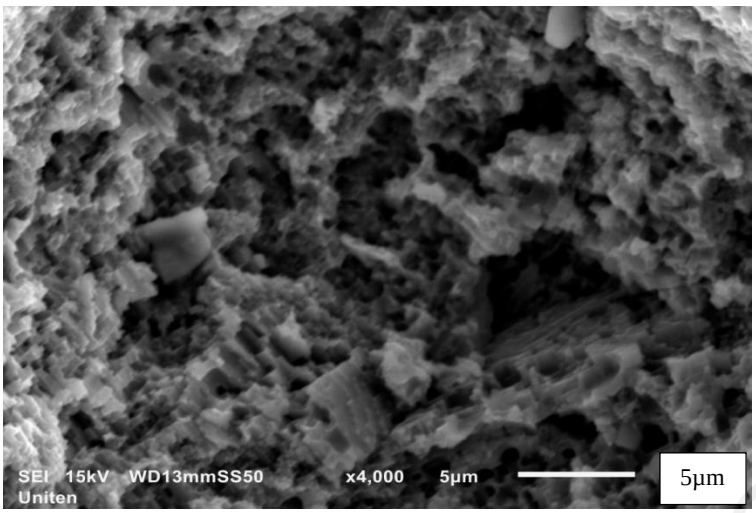

Figure 4.11: Sample P etched subject to reaction temperature of 80°C

It can be observed from Figure 4.9 that at 50°C (Sample J), an average amount of craters containing flakes are randomly distributed over the aluminium fin surface. Anyhow, there was not any flower-like microstructure present on the surface. It is seen that for sample N etched at 70°C, aluminium palmitate, $Al(CH_3(CH_2)_{12}COO)_3$ micro-nano flakes embody a large area of the aluminium surface consistently and compactly (Figure 4.9) giving the best CA. The orientations of most flakes were in the horizontal and downward direction and geometry was similar to cauliflower florets.

Besides that, interconnected porous structures were joined together by two or more flakes. Overall, there are no isolated flakes/etched pores in the surface, unlike the surface of sample J, which possessed such structures. For sample P prepared at reaction temperature of 80°C, the previously superhydrophobic contact angle values changed to a lower value of 132.2±1.3, implying that the wetting state was reverted back to Wenzel from Cassie-Baxter. Aluminium palmitate is a type of palmitic acid, a superhydrophobic end product from the reaction between metal (aluminium) and fatty acid (myristic acid).

As detected from Figure 4.10, repeated gaps with width greater than 1µm were formed on the top layer. When a droplet is placed onto the surface, it did not occupy the

spaces between micro and nano-structures, developing a composite interface comprising of solid and air (Jie at al., 2016). However, at this stage, droplets will protrude downward into micro-sized gaps due to surface curvature. At the point where protrusion depth is equivalent to the gap depths, water would be in contact with the underlying solid surface, leading to penetration into gaps (Victor, 2012). Therefore, CA is lowered to values related to the Wenzel state.

4.6 MYRISTIC ACID AND HYDROCHLORIC ACID IN ETHANOL SOLUTION AS ETCHANT

During the fabrication of surfaces with super-water-repellence, mainly two steps are involved, (i) forming hierarchical structures with a certain roughness through immersion in etchants and (ii) activation of this textured surface/lowering surface energy using fatty acids, such as myristic acid, lauric acid and stearic acid (Yao et al., 2011; Saleema et al., 2010). Through chemical etching, pores are formed at the surface, which hold air ensuring that water droplets are not in contact with the solid surface (Bhushan and Jung, 2011).

The reaction in this research requires an acidic medium (provided by HCl) to remove the natural oxide layer of the substrate partially. Another function of the acidic medium is ensuring that roughness produced through etching is not lost, as it assists in entrapment of air. According to Rezayi and Entezari (2016), etching in acidic medium also increases superhydrophobic stability. Fatty acid such as myristic acid is used in the experiments to lower the surface energy also. Similarly, works by Guo and Wang (2011) also employed simple immersion and surface energy reduction using stearic acid.

As two-step methods are time-consuming and tedious (Escobar and Llorca-Isern, 2014), this study was aimed at developing a facile single-step method. In single-step methods, samples with an original roughness need a particular terminal roughness to achieve superhydrophobicity in a single reaction.

4.6.1 Chemical Reactions during modification and formation of Superhydrophobic Surface

The technique used in this research is generating micro-rough surface via chemical etching, then formation of water-repellent surface by subsequent fixation of hydrophobic organic compounds. In the process of converting the as-received aluminium samples to super hydrophobic surfaces, a series of chemical reactions occur.

An acidic medium was provided by HCl to improve the oxide layer removal process. The protective aluminium oxide which exists naturally on the sample before chemical modification may partially dissolve because of the presence of Cl^- ions from the ethanol solution of HCl. The chemical reactions that are explained in the following sections are illustrated in Figure 4.12.

Furthermore, H^+ cation and Cl^- anion are highly oxidative, facilitating homogenous pitting corrosion on the aluminium surface (Mazhar et al., 2001). Cl^- ions attack and dissolve high surface energy areas such as grain boundaries and dislocations along glide plane to release Al^{3+}, forming nano-scale structures (Qian and Shen, 2005). Simultaneously, hydrogen ions cause the formation of hydrogen gas and also react with oxygen to form water (Zhang et al., 2011).

Now that the aluminium surface is exposed to the etchant, a redox reaction occurs according the equation below:

$2Al_{metal} + 6HCl \rightarrow 2AlCl_3 + 3H_2$ ---------- Equation 4.1

$O_2 + 4H^+ + 4e \rightarrow 2H_2O$ ---------- Equation 4.2

The released Al^{3+} ion reacts with the tetradecanoate ion, $CH_3(CH_2)_{12}COO^-$ from myristic acid to form a compound called aluminium palmitate in an addition reaction as shown in the equation below :

$Al^{3+} + CH_3(CH_2)_{12}COO^- \rightarrow Al(CH_3(CH_2)_{12}COO)_3$ ---------- Equation 4.3

The etching reaction using myristic acid and ethanol solution of hydrochloric acid produced pits on the surface and the resultant compound on the surface is aluminium palmitate, which is the bright nano-particle. According to Cassie theory (Cassie and Baxter, 1944), aluminium palmitate sticks to the hydrophobic tails on the existing rough structure which encourages non-wetting feature on the previously hydrophilic aluminium substrate (CA=70º).

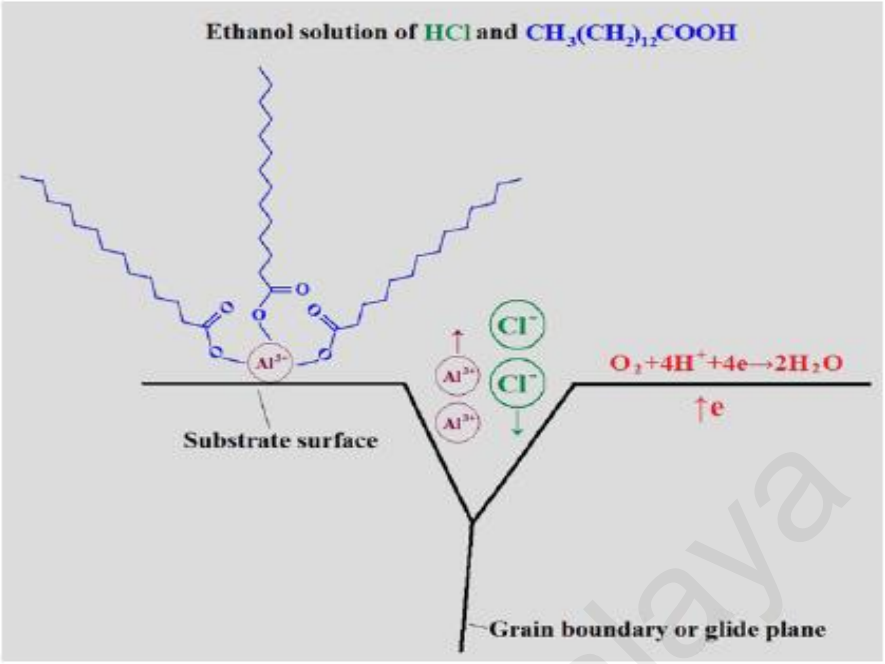

Figure 4.12: Illustration of superhydrophobic surface preparation on Al substrates using the single-step process adapted from Zhang et al. (2011)

4.7 WETTABILITY ANALYSIS OF SHP SURFACE

The as-received aluminium sample often exists with a native oxidized layer (He et al., 2009). The bare sample has a CA of 70º while the maximum CA of 159.4º is obtained after chemical treatment. The relationship between wettability and heterogeneous surfaces can be explained using the Cassie and Baxter theory, which propose that water droplets do not infiltrate into the grooves, but merely suspend on the micro- and nano-scale film. Hence, droplets do not easily adhere to the surface and slide off easily from the surface with even the slightest inclination or vibration.

Research by Yong et al. (2008) states that the air trapped in the structures formed on the surface due to chemical treatment plays a vital role in increasing the CA, hindering the droplet from penetrating the surface. The Cassie-Baxter equations below

can describe the contact angle of the rough surface composed of solid and air after chemical treatment (Yuzhen et al., 1975):

$\cos \theta_{rough} = f_s \cos \theta_{flat} - f_a$ ---------- Equation 4.4

$f_s + f_a = 1$ ---------- Equation 4.5

where f_s and f_a is the area ratio of the solid surface that contacts water and area ratio of air and solid surface respectively. θ_{rough} is the CA of the rough surface after chemical etching and the maximum value achieved of 159.4 ° is taken. θ_{flat} is equivalent to 70º, which is the angle on the flat bare aluminium sample before experimentation.

Substituting these values and solving equations 1 and 2, f_s value is 0.048. Consequently, the f_a value is 0.952, implying that 95.2% of the surface area is made of air-solid interface. Since the air-solid interface dominates the surface, it is hard for droplets to adhere to the surface. Hence, it can be concluded that trapped air plays an important role in lowering the adhesion force between the surface and water droplets.

4.8 EDS ANALYSIS

Energy dispersive X-ray spectrum (EDS) was used to analyse the micro-zone constitution of the bare Al3102 fin surface (t=0.1mm) and sample B, which exhibited the highest CA among all samples experimented (159.4º±1.1º). Figure 4.13 shows that Al and O exist on the surface, indicating an oxidized layer, naturally existing on the surface. There are also minute amounts of C and Si, implying that the surface contains impurities because the sample was not sanded prior to experimentation.

From the EDS image in Figure 4.13, it is seen that the element C has increased from 2.6% to 5.9% after chemical modification. Its presence is inferred to be mainly from the bonding of the tetradecanoate ion, $CH_3(CH_2)_{12}COO^-$ with the Al^{3+} on the

aluminium surface (Yin et al., 2008). During the etching process, the freed aluminium ions are instantly captured by coordination with *n*-tetradecanoic acid molecules, forming aluminium palmitate. The small percentage of Fe is due to the presence of impurities.

Table 4.6: EDS results of bare aluminium sample and treated superhydrophobic sample B

Sample	Element	wt%	at%
Bare Al3102 fin	AlK	94.3	86.09
	CK	2.6	11.58
	OK	2.7	2.17
	SiK	0.3	0.16
Sample B	AlK	90.6	83.81
	CK	5.9	11.39
	OK	2.91	4.54
	FeK	0.59	0.26

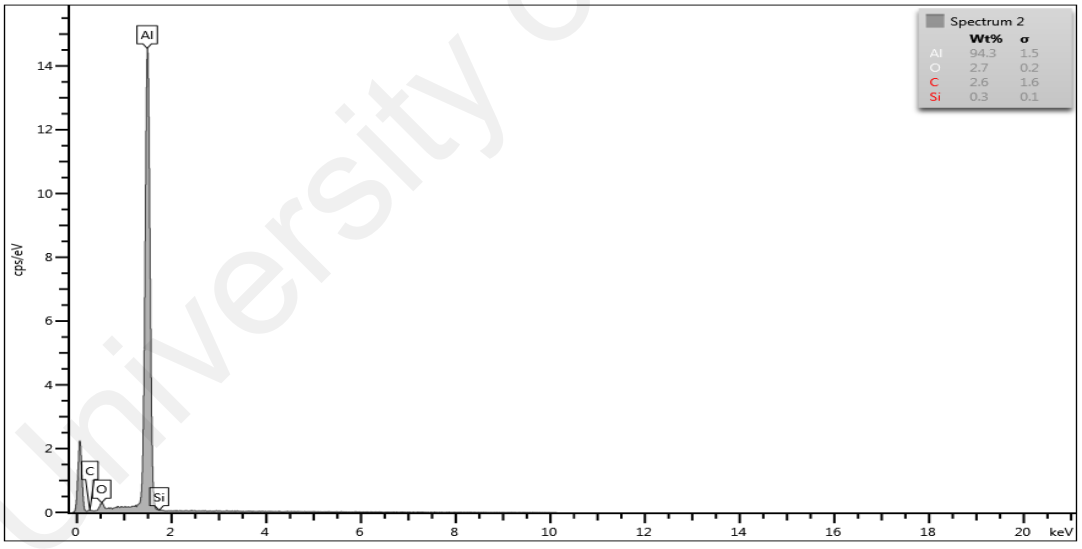

Figure 4.13: EDS results of bare Al3102 fin

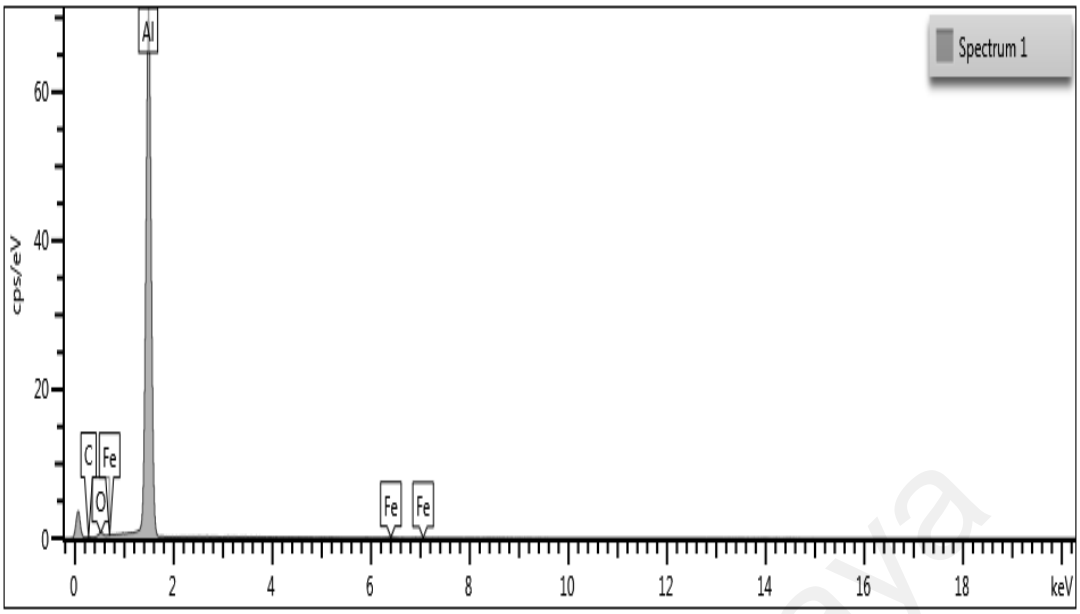

Figure 4.14: EDS results of sample B with CA =159.4º±1.1º

CHAPTER 5

CONCLUSION

For this study on rough surface preparation for superhydrophobicity, parameters such as etching time, myristic acid concentration, type and thickness of aluminium substrate and reaction temperature has been investigated. It is concluded that the best etching time is 15 minutes giving the highest CA of 159.4º±1.1º and the best myristic acid concentration is 3 g/l producing greatest CA of 156.9º±1.5º.

Apart from that, compared to foil and plate, aluminium fin with thickness of 0.1 mm (highest CA = 159.3º±1.0º) is the most conducive for superhydrophobicity. Hence, aluminium 3102 material can be used as fin material for fin-and-tube heat exchangers which are commonly used in air conditioners and heat pumps. Lastly, the best reaction temperature for chemical etching process is 70ºC as a superhydrophobic surface was fabricated at this temperature with CA of 152.2º±2.0º.

Among all four experiments conducted, the maximum contact angle obtained is 159.4º from experiment 1 at etching time of 15 minutes using aluminium fin (thickness = 0.1mm) as substrate, myristic acid concentration of 3 g/l and reaction temperature of 70ºC. Using this as the CA value after chemical treatment and CA value of 70º of bare aluminium sample, wettability analysis was done according to the Cassie-Baxter model. Calculations revealed that 95.2% of the surface area is made up of solid-air interface, implying that only 4.8% of the surface is in contact with the water droplet.

This indicates that a superhydrophobic surface with excellent non-wetting feature has indeed been produced. SEM images exhibited that the fabricated surfaces had dual roughness with micro and nano-scale structures, which are primarily

responsible for superhydrophobicity. EDS analysis was used to compared the elements present on the sample before and after treatment. The increase in carbon percentage after chemical modification is caused by bonding of the tetradecanoate ion, $CH_3(CH_2)_{12}COO^-$ with free aluminium ions on the surface.

As the result of etching on Al samples using myristic acid and ethanol solution of HCl, aluminium palmitate has been formed. In a nutshell, this project has proved that long-chain fatty acids can be used for superhydrophobic fabrication via one-step chemical etching due to its due hydrophobic tails; this one-step solution-immersion technique is low-cost, quick and simple to adopt. It is an economically feasible approach for large-scale fabrication of superhydrophobic Al surfaces.

Based on the reviews and research done for this project, it is evident there is a research gap in terms of type or thickness of metal substrate which is optimum for maximum contact angle. Knowing the ideal film thickness is important so that unnecessary usage of material can be avoided. For further cost-reduction, research could be done on chemical etching using only a single reagent instead of two or more.

Most studies in this field suggest only superficial results for wettability and slip and only the contact angle is presented as the outcome of research. It is recommended that the contact angel hysteresis and sliding also be measured for the classification of a material's wetting state. Despite being vital to this topic, the roughness concept is had to be modelled on various substrates found in nature or fabricated in the laboratory. Hence, additional models will be needed to correlate hysteresis to roughness.

REFERENCES

Analysis, S. (2016). A facile method for fabrication of superhydrophobic coating on aluminium alloy A facile method for fabrication of superhydrophobic coating on aluminium alloy. . doi:10.1002/sia.3823

Bayat, A., Ebrahimi, M., Nourmohammadi, A., & Moshfegh, A. Z. (2015). Applied Surface Science Wettability properties of PTFE / ZnO nanorods thin film exhibiting UV-resilient superhydrophobicity. *Applied Surface Science*, *341*, 92–99. doi:10.1016/j.apsusc.2015.02.197

Beckford, S., & Zou, M. (2011). Micro / nano engineering on stainless steel substrates to produce superhydrophobic surfaces. *Thin Solid Films*, *520*(5), 1520–1524. doi:10.1016/j.tsf.2011.05.081

Belaud, V., Valette, S., Stremsdoerfer, G., Bigerelle, M., & Benayoun, S. (2015). Tribology International Wettability versus roughness : Multi-scales approach. *Tribiology International*, *82*, 343–349. doi:10.1016/j.triboint.2014.07.002

Berendjchi, A., Khajavi, R., & Yazdanshenas, M. E. (2011). Fabrication of superhydrophobic and antibacterial surface on cotton fabric by doped silica - based sols with nanoparticles of copper. *Nanoscale Research Letters*, *6*(1), 594–594. doi:10.1186/1556-276X-6-594

Bharathidasan, T., Kumar, S. V., Bobji, M. S., Chakradhar, R. P. S., & Basu, B. J. (2014). Applied Surface Science Effect of wettability and surface roughness on ice-adhesion strength of hydrophilic , hydrophobic and superhydrophobic surfaces. *Applied Surface Science*, *314*, 241–250. doi:10.1016/j.apsusc.2014.06.101

Bhushan, B., & Jung, Y. C. (2011). Natural and biomimetic artificial surfaces for superhydrophobicity, self-cleaning, low adhesion, and drag reduction. *Progress in Materials Science*, *56*(1), 1–108. doi:10.1016/j.pmatsci.2010.04.003

Bhushan, B., Jung, Y. C., Niemietz, A., & Koch, K. (2009). Lotus-like biomimetic hierarchical structures developed by the self-assembly of tubular plant waxes. *Langmuir*, *25*(3), 1659–1666. doi:10.1021/la802491k

Bravo, J., Zhai, L., Wu, Z., Cohen, R. E., & Rubner, M. F. (2007). Transparent superhydrophobic films based on silica nanoparticles. *Langmuir*, *23*(13), 7293–7298. doi:10.1021/la070159q

Cassie, B. D. (1944). wettability of Of porous surfaces,. 546–551.

Charyangi, D., Silva, R. M. D., & Silva, K. M. N. D. (2016). Applied Surface Science Double layer approach to create durable superhydrophobicity on cotton fabric using nano silica and auxiliary non fluorinated materials. *Applied Surface Science*, *360*, 777–788. doi:10.1016/j.apsusc.2015.11.068

Chen, T., Ge, S., Liu, H., Sun, Q., Zhu, W., & Yan, W. (2015). Applied Surface Science Fabrication of low adhesive superhydrophobic surfaces using nano Cu / Al 2 O 3 Ni – Cr composited electro-brush plating. *Applied Surface Science*, *356*, 81–90. doi:10.1016/j.apsusc.2015.08.045

Chen, X., Kong, L., Dong, D., Yang, G., Yu, L., Chen, J., & Zhang, P. (2009). Synthesis and characterization of superhydrophobic functionalized Cu(OH)2 nanotube arrays on copper foil. *Applied Surface Science*, *255*(7), 4015–4019. doi:10.1016/j.apsusc.2008.10.104

Cho, Y. J., Jang, H., Lee, K. S., & Kim, D. R. (2015). Direct growth of cerium oxide nanorods on diverse substrates for superhydrophobicity and corrosion resistance. *Applied Surface Science*, *340*, 96–101. doi:10.1016/j.apsusc.2015.02.138

Cui, Z., Yin, L., Wang, Q., Ding, J., & Chen, Q. (2009). A facile dip-coating process for preparing highly durable superhydrophobic surface with multi-scale structures on paint films. *Journal of Colloid and Interface Science*, *337*(2), 531–537. doi:10.1016/j.jcis.2009.05.061

Das, A., Schutzius, T. M., Bayer, I. S., & Megaridis, C. M. (2011). Superoleophobic and conductive carbon nanofiber / fluoropolymer composite films. *Carbon*, *50*(3), 1346–1354. doi:10.1016/j.carbon.2011.11.006

Escobar, A. M., & Llorca-Isern, N. (2014). Superhydrophobic coating deposited directly on aluminum. *Applied Surface Science*, *305*, 774–782. doi:10.1016/j.apsusc.2014.03.196

Escobar, A. M., Llorca-isern, N., & Rius-ayra, O. (2016). Materials Characterization Identi fi cation of the mechanism that confers superhydrophobicity on 316L stainless steel. *Materials Characterization*, *111*, 162–169. doi:10.1016/j.matchar.2015.11.026

Fu, Y., Yu, H., Sun, Q., Li, G., & Liu, Y. (2016). Testing of the superhydrophobicity of a zinc oxide nanorod array coating on wood surface prepared by hydrothermal treatment Testing of the superhydrophobicity of a zinc oxide nanorod array coating on wood surface prepared by hydrothermal treatment. . doi:10.1515/hf-2011-0261

Ganesan, P., Vanaki, S. M., Thoo, K. K., & Chin, W. M. (2016). Air-side heat transfer characteristics of hydrophobic and super-hydrophobic fin surfaces in heat exchangers: A review. *International Communications in Heat and Mass Transfer*, *74*, 27–35. doi:10.1016/j.icheatmasstransfer.2016.02.017

Gokhale, S. J., Plawsky, J. L., & Wayner, P. C. (2003). Experimental investigation of contact angle, curvature, and contact line motion in dropwise condensation and evaporation. *Journal of Colloid and Interface Science*, *259*(2), 354–366. doi:10.1016/S0021-9797(02)00213-8

Gong, D., Long, J., Fan, P., Jiang, D., Zhang, H., & Zhong, M. (2015). Applied Surface Science Thermal stability of micro – nano structures and superhydrophobicity of polytetrafluoroethylene films formed by hot embossing via a picosecond laser ablated template. *Applied Surface Science*, *331*, 437–443. doi:10.1016/j.apsusc.2015.01.102

Guan, H., Han, Z., Cao, H., Niu, S., Qian, Z., Ye, J., & Ren, L. (2015). Characterization of Multi-scale Morphology and Superhydrophobicity of Water Bamboo Leaves and Biomimetic Polydi- methylsiloxane (PDMS) Replicas. *Journal of Bionic Engineering*, *12*(4), 624–633. doi:10.1016/S1672-6529(14)60152-9

Guo, Z., Fang, J., Wang, L., & Liu, W. (2007). Fabrication of superhydrophobic copper by wet chemical reaction. , *515*, 7190–7194. doi:10.1016/j.tsf.2007.02.100

Guo, F., Su, X., Hou, G., & Li, P. (2012). Colloids and Surfaces A : Physicochemical and Engineering Aspects Bioinspired fabrication of stable and robust superhydrophobic steel surface with hierarchical flowerlike structure. *Colloids and Surfaces A: Physicochemical and Engineering Aspects*, *401*, 61–67. doi:10.1016/j.colsurfa.2012.03.013

Hao, X., Wang, L., Lv, D., Wang, Q., Li, L., He, N., & Lu, B. (2015). Applied Surface Science Fabrication of hierarchical structures for stable superhydrophobicity on metallic planar and cylindrical inner surfaces. *Applied Surface Science*, *325*, 151–159. doi:10.1016/j.apsusc.2014.11.014

Hashemzadeh, M., Raeissi, K., Ashrafizadeh, F., & Khorsand, S. (2015). Effect of ammonium chloride on microstructure, super-hydrophobicity and corrosion resistance of nickel coatings. *Surface and Coatings Technology*, *283*, 318–328. doi:10.1016/j.surfcoat.2015.11.008

He, T., Wang, Y., Zhang, Y., lv, Q., Xu, T., & Liu, T. (2009). Super-hydrophobic surface treatment as corrosion protection for aluminum in seawater. *Corrosion Science*, *51*(8), 1757–1761. doi:10.1016/j.corsci.2009.04.027

He, Y., Jiang, C., Yin, H., & Yuan, W. (2011). Applied Surface Science Tailoring the wettability of patterned silicon surfaces with dual-scale pillars : From hydrophilicity to superhydrophobicity. *Applied Surface Science*, *257*(17), 7689–7692. doi:10.1016/j.apsusc.2011.04.009

Hong, Y. C., Cho, S. C., Shin, D. H., Lee, S. H., & Uhm, H. S. (2008). A facile method for the fabrication of super-hydrophobic surfaces and their resulting wettability. *Scripta Materialia*, *59*(7), 776–779. doi:10.1016/j.scriptamat.2008.06.012

Hosono, E., Fujihara, S., Honma, I., & Zhou, H. (2005). Superhydrophobic perpendicular nanopin film by the bottom-up process. *Journal of the American Chemical Society*, *127*(39), 13458–13459. doi:10.1021/ja053745j

Hsieh, C., Chen, J., Kuo, R., Lin, T., & Wu, C. (2005). Influence of surface roughness on water- and oil-repellent surfaces coated with nanoparticles. , *240*, 318–326. doi:10.1016/j.apsusc.2004.07.016

Hsieh, C., Chen, W., & Wu, F. (2008). Fabrication and superhydrophobicity of fluorinated carbon fabrics with micro / nanoscaled two-tier roughness. , *6*, 3–9. doi:10.1016/j.carbon.2008.04.026

Hsieh, C., Chen, W., Wu, F., & Hung, W. (2010). Diamond & Related Materials Superhydrophobicity of a three-tier roughened texture of microscale carbon fabrics decorated with silica spheres and carbon nanotubes. *Diamond & Related Materials*, *19*(1), 26–30. doi:10.1016/j.diamond.2009.10.017

Hsieh, C., Wu, F., & Chen, W. (2009). Surface & Coatings Technology Super water- and oil-repellencies from silica-based nanocoatings. *Surface & Coatings Technology*, *203*(22), 3377–3384. doi:10.1016/j.surfcoat.2009.04.025

Hsieh, C., Wu, F., & Yang, S. (2008). Surface & Coatings Technology Superhydrophobicity from composite nano / microstructures : Carbon fabrics coated with silica nanoparticles. , *202*, 6103–6108. doi:10.1016/j.surfcoat.2008.07.006

Il, Y., Sik, H., Seok, W., Seung, T., & Ho, W. (2009). Superhydrophobicity of cellulose triacetate fibrous mats produced by electrospinning and plasma treatment. *Carbohydrate Polymers*, *75*(2), 246–250. doi:10.1016/j.carbpol.2008.07.015

Jie, H., Xu, Q., Wei, L., & Min, Y. L. (2016). Etching and heating treatment combined approach for superhydrophobic surface on brass substrates and the consequent corrosion resistance. *Corrosion Science*, *102*, 251–258. doi:10.1016/j.corsci.2015.10.013

Jokinen, V., Suvanto, P., Garapaty, A. R., Lyytinen, J., & Koskinen, J. (2013). Colloids and Surfaces A : Physicochemical and Engineering Aspects Durable superhydrophobicity in embossed CYTOP fluoropolymer micro and nanostructures. *Colloids and Surfaces A: Physicochemical and Engineering Aspects*, *434*, 207–212. doi:10.1016/j.colsurfa.2013.05.061

Kermani, Z. (2005). Wettability of porous polydimethylsiloxane surface : morphology study. , *242*, 339–345. doi:10.1016/j.apsusc.2004.08.035

Kim, T., Tahk, D., & Lee, H. H. (2009). Wettability-Controllable Super Water- and Moderately Oil-Repellent Surface Fabricated by Wet Chemical Etching. , *25*(c), 6576–6579. doi:10.1021/la900106s

Koch, K., Bhushan, B., Jung, Y. C., & Barthlott, W. (2009). Fabrication of artificial Lotus leaves and significance of hierarchical structure for superhydrophobicity and low adhesion. *Soft Matter*, *5*(7), 1386–1386. doi:10.1039/b818940d

Korhonen, J. T., Huhtamäki, T., Ikkala, O., & Ras, R. H. A. (2013). Reliable measurement of the receding contact angle. *Langmuir*, *29*(12), 3858–3863. doi:10.1021/la400009m

Krasovitski, B., & Marmur, A. (2005). Drops down the hill: Theoretical study of limiting contact angles and the hysteresis range on a tilted plate. *Langmuir*, *21*(9), 3881–3885. doi:10.1021/la0474565

Kwon, Y., Patankar, N., Choi, J., & Lee, J. (2009). Design of surface hierarchy for extreme hydrophobicity. *Langmuir*, *25*(11), 6129–6136. doi:10.1021/la803249t

Lakshmi, R. V., & Basu, B. J. (2009). Journal of Colloid and Interface Science Fabrication of superhydrophobic sol – gel composite films using hydrophobically modified colloidal zinc hydroxide. *Journal of Colloid And Interface Science*, *339*(2), 454–460. doi:10.1016/j.jcis.2009.07.064

Lakshmi, R. V., Bharathidasan, T., Bera, P., & Basu, B. J. (2012). Surface & Coatings Technology Fabrication of superhydrophobic and oleophobic sol – gel nanocomposite coating. *Surface & Coatings Technology*, *206*(19-20), 3888–3894. doi:10.1016/j.surfcoat.2012.03.044

Latthe, S. S., & Rao, A. V. (2012). Surface & Coatings Technology Superhydrophobic SiO 2 micro-particle coatings by spray method. *Surface & Coatings Technology*, *207*, 489–492. doi:10.1016/j.surfcoat.2012.07.055

Li, Y., Cai, W., Duan, G., Cao, B., Sun, F., & Lu, F. (2005). Superhydrophobicity of 2D ZnO ordered pore arrays formed by solution-dipping template method. *Journal of Colloid and Interface Science*, *287*(2), 634–639. doi:10.1016/j.jcis.2005.02.010

Li, W., & Amirfazli, A. (2008). Hierarchical structures for natural superhydrophobic surfaces. *Soft Matter*, *4*(3), 462–466. doi:10.1039/B715731B

Liang, J., Hu, Y., Wu, Y., & Chen, H. (2014). Surface & Coatings Technology Facile formation of superhydrophobic silica-based surface on aluminum substrate with tetraethylorthosilicate and vinyltriethoxysilane as co-precursor and its corrosion resistant performance in corrosive NaCl aqueous solution. *Surface & Coatings Technology*, *240*, 145–153. doi:10.1016/j.surfcoat.2013.12.028

Liao, R., Zuo, Z., Guo, C., Yuan, Y., & Zhuang, A. (2014). Fabrication of superhydrophobic surface on aluminum by continuous chemical etching and its anti-icing property. *Applied Surface Science*, *317*, 701–709. doi:10.1016/j.apsusc.2014.08.187

Li, J., Du, F., Liu, X., Jiang, Z., & Ren, L. (2011). Superhydrophobicity of Bionic Alumina Surfaces Fabricated by Hard Anodizing. *Journal of Bionic Engineering*, *8*(4), 369–374. doi:10.1016/S1672-6529(11)60042-5

Lim, S., Horiuchi, H., Nikolov, A. D., & Wasan, D. (2015). Nanofluids alter the surface wettability of solids. *Langmuir*, *31*(21), 5827–5835. doi:10.1021/acs.langmuir.5b00799

Li, X.-M., Reinhoudt, D., & Crego-Calama, M. (2007). What do we need for a superhydrophobic surface? A review on the recent progress in the preparation of superhydrophobic surfaces. *Chemical Society reviews*, *36*(8), 1350–1368. doi:10.1039/b602486f

Liu, B., Wang, W., Jiang, G., Mei, X., Wang, Z., Wang, K., & Cui, J. (2016). Study on hierarchical structured PDMS for surface super-hydrophobicity using imprinting with ultrafast laser structured models. *Applied Surface Science*, *364*, 528–538. doi:10.1016/j.apsusc.2015.12.190

Liu, P., Cao, L., Zhao, W., Xia, Y., Huang, W., & Li, Z. (2015). Insights into the superhydrophobicity of metallic surfaces prepared by electrodeposition involving spontaneous adsorption of airborne hydrocarbons. *Applied Surface Science*, *324*, 576–583. doi:10.1016/j.apsusc.2014.10.170

Liu, Y., Liu, J., Li, S., Wang, Y., Han, Z., & Ren, L. (2015). Colloids and Surfaces A : Physicochemical and Engineering Aspects One-step method for fabrication of biomimetic superhydrophobic surface on aluminum alloy. *Colloids and Surfaces A: Physicochemical and Engineering Aspects*, *466*, 125–131. doi:10.1016/j.colsurfa.2014.11.017

Liu, L., Liu, W., Chen, R., Li, X., & Xie, X. (2015). Hierarchical growth of Cu zigzag microstrips on Cu foil for superhydrophobicity and corrosion resistance. *Chemical Engineering Journal*, *281*, 804–812. doi:10.1016/j.cej.2015.07.028

Liu, M., Qing, Y., Wu, Y., Liang, J., & Luo, S. (2015). Applied Surface Science Facile fabrication of superhydrophobic surfaces on wood substrates via a one-step hydrothermal process. *Applied Surface Science*, *330*, 332–338. doi:10.1016/j.apsusc.2015.01.024

Liu, T., Yin, Y., Chen, S., Chang, X., & Cheng, S. (2007). Super-hydrophobic surfaces improve corrosion resistance of copper in seawater. *Electrochimica Acta*, *52*(11), 3709–3713. doi:10.1016/j.electacta.2006.10.059

Liu, L., Zhao, J., Zhang, Y., Zhao, F., & Zhang, Y. (2011). Journal of Colloid and Interface Science Fabrication of superhydrophobic surface by hierarchical growth of lotus-leaf-like boehmite on aluminum foil. *Journal of Colloid And Interface Science*, *358*(1), 277–283. doi:10.1016/j.jcis.2011.02.036

Long, J., Zhong, M., Zhang, H., & Fan, P. (2015). Journal of Colloid and Interface Science Superhydrophilicity to superhydrophobicity transition of picosecond laser microstructured aluminum in ambient air. *JOURNAL OF COLLOID AND INTERFACE SCIENCE*, *441*, 1–9. doi:10.1016/j.jcis.2014.11.015

Mahadik, S. A., Kavale, M. S., Mukherjee, S. K., & Rao, A. V. (2010). Applied Surface Science Transparent Superhydrophobic silica coatings on glass by sol – gel method. *Applied Surface Science*, *257*(2), 333–339. doi:10.1016/j.apsusc.2010.06.062

Ma, M., & Hill, R. M. (2006). Superhydrophobic surfaces. , *11*, 193–202. doi:10.1016/j.cocis.2006.06.002

Mansoor, M. A., Ehsan, M. A., McKee, V., Huang, N.-M., Ebadi, M., Arifin, Z., … Mazhar, M. (2013). Hexagonal structured Zn(1−x)CdxO solid solution thin films: synthesis, characterization and applications in photoelectrochemical water splitting. *Journal of Materials Chemistry A*, *1*(17), 5284–5284. doi:10.1039/c3ta10558j

Mazhar, A. A., Arab, S. T., & Noor, E. A. (2001). The role of chloride ions and pH in the corrosion and pitting of Al-Si alloys. *Journal of Applied Electrochemistry*, *31*(10), 1131–1140. doi:10.1023/A:1012039804089

Meng, L., Yop, K., & Park, S. (2014). Journal of Industrial and Engineering Chemistry Enhancement of superhydrophobicity and conductivity of carbon nanofibers-coated glass fabrics. *Journal of Industrial and Engineering Chemistry*, *20*(4), 1672–1676. doi:10.1016/j.jiec.2013.08.015

Nakajima, A., Abe, K., U, K. H., & Watanabe, T. (2000). Preparation of hard super-hydrophobic films with visible light transmission.

Nimittrakoolchai, O., & Supothina, S. (2008). Deposition of organic-based superhydrophobic films for anti-adhesion and self-cleaning applications. , *28*, 947–952. doi:10.1016/j.jeurceramsoc.2007.09.025

Nosonovsky, M., & Bhushan, B. (2007). Hierarchical roughness optimization for biomimetic superhydrophobic surfaces. *Ultramicroscopy*, *107*(10-11), 969–979. doi:10.1016/j.ultramic.2007.04.011

Nosonovsky, M., & Bhushan, B. (2009). Superhydrophobic surfaces and emerging applications: Non-adhesion, energy, green engineering. *Current Opinion in Colloid and Interface Science*, *14*(4), 270–280. doi:10.1016/j.cocis.2009.05.004

Pacifico, J., Endo, K., Morgan, S., & Mulvaney, P. (2006). Superhydrophobic effects of self-assembled monolayers on micropatterned surfaces: 3-D arrays mimicking the Lotus Leaf. *Langmuir*, *22*(26), 11072–11076. doi:10.1021/la060925d

Pan, L., Dong, H., & Bi, P. (2010). Facile preparation of superhydrophobic copper surface by HNO3 etching technique with the assistance of CTAB and ultrasonication. *Applied Surface Science*, *257*(5), 1707–1711. doi:10.1016/j.apsusc.2010.09.001

Park, J. S., Kihm, K. D., Kim, H., Lim, G., Cheon, S., & Lee, J. S. (2014). Wetting and evaporative aggregation of nanofluid droplets on CVD-synthesized hydrophobic graphene surfaces. *Langmuir*, *30*(28), 8268–8275. doi:10.1021/la404854z

Park, J., Lim, H., Kim, W., & Soo, J. (2011). Journal of Colloid and Interface Science Design and fabrication of a superhydrophobic glass surface with micro-network of nanopillars. *Journal of Colloid And Interface Science*, *360*(1), 272–279. doi:10.1016/j.jcis.2011.04.047

Qian, B., & Shen, Z. (2005). Fabrication of superhydrophobic surfaces by dislocation-selective chemical etching on aluminum, copper, and zinc substrates. *Langmuir*, *21*(20), 9007–9009. doi:10.1021/la051308c

Rezayi, T., & Entezari, M. H. (2016). Toward a durable superhydrophobic aluminum surface by etching and ZnO nanoparticle deposition. *Journal of Colloid and Interface Science*, *463*, 37–45. doi:10.1016/j.jcis.2015.10.029

Ruan, M., Li, W., Wang, B., Luo, Q., Ma, F., & Yu, Z. (2012). Optimal conditions for the preparation of superhydrophobic surfaces on al substrates using a simple etching approach. *Applied Surface Science*, *258*(18), 7031–7035. doi:10.1016/j.apsusc.2012.03.159

Ruan, M., Li, W., Wang, B., Deng, B., Ma, F., & Yu, Z. (2013). Preparation and Anti-icing Behavior of Superhydrophobic Surfaces on Aluminum Alloy Substrates.

Saleema, N., & Farzaneh, M. (2008). Thermal effect on superhydrophobic performance of stearic acid modified ZnO nanotowers. , *254*, 2690–2695. doi:10.1016/j.apsusc.2007.10.004

Saleema, N., Sarkar, D. K., Paynter, R. W., & Chen, X. G. (2010). Superhydrophobic aluminum alloy surfaces by a novel one-step process. *ACS Applied Materials and Interfaces*, *2*(9), 2500–2502. doi:10.1021/am100563u

Samsudin, E. M., Soo, C. W., Abd Hamid, S. B., Basiron, W. J., Lai, C. W., Lai, C. W., … Juan, J. C. (2015). Synthesis and Characterization of TiO2 Nanoparticles via Alternative Sol-Gel Preparation Routes. *Advanced Materials Research*, *1087*, 191–196. doi:10.4028/www.scientific.net/AMR.1087.191

Shang, H. M., Wang, Y., Limmer, S. J., Chou, T. P., Takahashi, K., & Cao, G. Z. (2005). Optically transparent superhydrophobic silica-based films. , *472*, 37–43. doi:10.1016/j.tsf.2004.06.087

Shi, X., Nguyen, T. A., Suo, Z., Wu, J., Gong, J., & Avci, R. (2012). Electrochemical and mechanical properties of superhydrophobic aluminum substrates modified with nano-silica and fluorosilane. *Surface and Coatings Technology*, *206*(17), 3700–3713. doi:10.1016/j.surfcoat.2012.02.058

Sommers, A. D., Yu, R., Okamoto, N. C., & Upadhyayula, K. (2012). Condensate drainage performance of a plain fin-and-tube heat exchanger constructed from anisotropic micro-grooved fins. *International Journal of Refrigeration*, *35*(6), 1766–1778. doi:10.1016/j.ijrefrig.2012.05.006

Song, W., Zhang, J., Xie, Y., Cong, Q., & Zhao, B. (2009). Large-area unmodified superhydrophobic copper substrate can be prepared by an electroless replacement deposition. *Journal of Colloid and Interface Science*, *329*(1), 208–211. doi:10.1016/j.jcis.2008.09.059

Sookhakian, M., Amin, Y. M., Basirun, W. J., Tajabadi, M. T., & Kamarulzaman, N. (2014). Synthesis, structural, and optical properties of type-II ZnO-ZnS core-shell nanostructure. *Journal of Luminescence*, *145*, 244–252. doi:10.1016/j.jlumin.2013.07.032

Srinivasan, S., Chhatre, S. S., Mabry, J. M., Cohen, R. E., & Mckinley, G. H. (2011). Solution spraying of poly (methyl methacrylate) blends to fabricate microtextured , superoleophobic surfaces. *Polymer*, *52*(14), 3209–3218. doi:10.1016/j.polymer.2011.05.008

Surface, S. (2004). A Lotus-Leaf-like Superhydrophobic Surface: A Porous Microsphere/Nanofiber Composite Film Prepared by Electrohydrodynamics - Jiang - 2004 - Angewandte Chemie International Edition - Wiley Online Library. 4438–4441. doi:10.1002/ange.200460333

Tarrade, J., Darmanin, T., Taffin, E., Givenchy, D., Guittard, F., Debarnot, D., & Poncin-epaillard, F. (2014). Applied Surface Science Texturation and superhydrophobicity of polyethylene terephthalate thanks to plasma technology. *Applied Surface Science*, *292*, 782–789. doi:10.1016/j.apsusc.2013.12.051

Thieme, M., Streller, F., Simon, F., Frenzel, R., & White, A. J. (2013). Superhydrophobic aluminium-based surfaces: Wetting and wear properties of different CVD-generated coating types. *Applied Surface Science*, *283*, 1041–1050. doi:10.1016/j.apsusc.2013.07.065

Tian, L., Yuanyuan, Z., Yingying, M., & Ran, H. (2015). Applied Clay Science Fabrication of functional silver loaded montmorillonite / polycarbonate with superhydrophobicity. *Applied Clay Science*, *118*, 337–343. doi:10.1016/j.clay.2015.10.016

Vafaei, S., Wen, D., & Borca-Tasciuc, T. (2011). Nanofluid surface wettability through asymptotic contact angle. *Langmuir*, *27*(6), 2211–2218. doi:10.1021/la104254a

Valipour, N. M., Birjandi, F. C., & Sargolzaei, J. (2014). Colloids and Surfaces A : Physicochemical and Engineering Aspects Super-non-wettable surfaces : A review. *Colloids and Surfaces A: Physicochemical and Engineering Aspects*, *448*(43), 93–106. doi:10.1016/j.colsurfa.2014.02.016

Valipour, N., Sargolzaei, J., & Shahtahmassebi, N. (2013). Surface & Coatings Technology Super-liquid-repellent coating on the carbon steel surface. *Surface & Coatings Technology*, *235*, 241–249. doi:10.1016/j.surfcoat.2013.07.039

Victor, J. J. (2012). BIOLOGY INSPIRED NANO-MATERIALS : SUPERHYDROPHOBIC SURFACES by. *Thesis*

Wagner, J. B., Timpe, O., Hamid, F. A., Trunschke, A., Wild, U., Su, D. S., … Schlögl, R. (2006). Surface texturing of Mo–V–Te–Nb–O x selective oxidation catalysts. *Topics in catalysis*, *38*(1), 51–58. doi:10.1007/s11244-006-0070-1

Wang, S., Li, Y. L., Zhao, H. L., Liang, H., Liu, B., & Pan, S. (2012). Preparation of porous monolayer film by immersing the stearic acid Langmuir-Blodgett monolayer on mica in salt solution. *Applied Surface Science*, *261*, 31–36. doi:10.1016/j.apsusc.2012.07.041

Wang, S., Liu, C., Liu, G., Zhang, M., Li, J., & Wang, C. (2011). Applied Surface Science Fabrication of superhydrophobic wood surface by a sol – gel process. *Applied Surface Science*, *258*(2), 806–810. doi:10.1016/j.apsusc.2011.08.100

Wang, J., Chen, J., Cao, S., Xia, S., Zhu, Y., & Xu, G. (2009). A facile route to prepare ZnO super-hydrophobic surface with hierarchical structure. , *117*, 183–186. doi:10.1016/j.matchemphys.2009.05.033

Wang, Q., Cui, Z., Xiao, Y., & Chen, Q. (2007). Stable highly hydrophobic and oleophilic meshes for oil-water separation. *Applied Surface Science*, *253*(23), 9054–9060. doi:10.1016/j.apsusc.2007.05.030

Wenzel, R. N. (1949). Surface Roughness and Contact Angle. *Journal of Psychosomatic Research*, *53*(9), 1466–1467. doi:10.1016/0022-3999(86)90018-8

Xiao, H., Hu, A., Hang, T., & Li, M. (2015). Electrodeposited nanostructured cobalt film and its dual modulation of both superhydrophobic property and adhesiveness. *Applied Surface Science*, *324*, 319–323. doi:10.1016/j.apsusc.2014.10.156

Xi, W., Qiao, Z., Zhu, C., Jia, A., & Li, M. (2009). The preparation of lotus-like super-hydrophobic copper surfaces by electroplating. *Applied Surface Science*, *255*(9), 4836–4839. doi:10.1016/j.apsusc.2008.12.012

Xue, L., Li, J., Fu, J., & Han, Y. (2009). Colloids and Surfaces A : Physicochemical and Engineering Aspects Super-hydrophobicity of silica nanoparticles modified with vinyl groups. , *338*, 15–19. doi:10.1016/j.colsurfa.2008.12.016

Xu, J., Li, M., Zhao, Y., & Lu, Q. (2007). Control over the hydrophobic behavior of polystyrene surface by annealing temperature based on capillary template wetting method. *Colloids and Surfaces A: Physicochemical and Engineering Aspects*, *302*(1-3), 136–140. doi:10.1016/j.colsurfa.2007.02.030

Yadav, K., Mehta, B. R., & Singh, J. P. (2015). Applied Surface Science Superhydrophobicity and enhanced UV stability in vertically standing indium oxide nanorods. *Applied Surface Science*, *346*, 361–365. doi:10.1016/j.apsusc.2015.03.012

Yang, H., Pi, P., Cai, Z. Q., Wen, X., Wang, X., Cheng, J., & Yang, Z. ru (2010). Facile preparation of super-hydrophobic and super-oleophilic silica film on stainless steel mesh via sol-gel process. *Applied Surface Science*, *256*(13), 4095–4102. doi:10.1016/j.apsusc.2010.01.090

Yanlong, S., Wu, Y., Jiajing, B., Xiaojuan, F., & Yongsheng, W. (2014). Surface & Coatings Technology Fabrication of fl ower-like copper fi lm with reversible superhydrophobicity – superhydrophilicity and anticorrosion properties. *Surface & Coatings Technology*, *253*, 148–153. doi:10.1016/j.surfcoat.2014.05.027

Yao, L., Zheng, M., Ma, L., Li, W., Li, M., & Shen, W. (2011). Self-assembly of diverse alumina architectures and their morphology-dependent wettability. *Materials Research Bulletin*, *46*(9), 1403–1408. doi:10.1016/j.materresbull.2011.05.018

Yao, L., & He, J. (2014). Progress in Materials Science Recent progress in antireflection and self-cleaning technology – From surface engineering to functional surfaces. *Progress in Materials Science*, *61*, 94–143. doi:10.1016/j.pmatsci.2013.12.003

Yilg, E., & Yilg, I. (2015). In fl uence of the average surface roughness on the formation of superhydrophobic polymer surfaces through spin-coating with hydrophobic fumed silica. , *62*, 118–128. doi:10.1016/j.polymer.2015.02.032

Yin, Y., Liu, T., Chen, S., Liu, T., & Cheng, S. (2008). Structure stability and corrosion inhibition of super-hydrophobic film on aluminum in seawater. *Applied Surface Science*, *255*(5 PART 2), 2978–2984. doi:10.1016/j.apsusc.2008.08.088

Yin, L., Wang, Y., Ding, J., Wang, Q., & Chen, Q. (2012). Applied Surface Science Water condensation on superhydrophobic aluminum surfaces with different low-surface-energy coatings. *Applied Surface Science*, *258*(8), 4063–4068. doi:10.1016/j.apsusc.2011.12.100

Yuan, J., & Jin, R. (2011). Direct Generation of Silica Nanowire-Based Thin Film on Various Substrates with Tunable Surface Nanostructure and Extreme Repellency toward Complex Liquids.

Yu, M., Gu, G., Meng, W., & Qing, F. (2007). Superhydrophobic cotton fabric coating based on a complex layer of silica nanoparticles and perfluorooctylated quaternary ammonium silane coupling agent. , *253*, 3669–3673. doi:10.1016/j.apsusc.2006.07.086

Yuzhen, L. V., Lefeng, W., Kaibo, M. A., You, Z., & Chengrong, L. I. (1975). Fabrication and Hydrophobic Properties of Coatings on Aluminum Foil #. 1–5.

Yüce, M. Y., & Demirel, A. L. (2008). The effect of nanoparticles on the surface hydrophobicity of polystyrene. *European Physical Journal B*, *64*(3-4), 493–497. doi:10.1140/epjb/e2008-00042-0

Zhai, L., Fevzi, C., Cohen, R. E., & Rubner, M. F. (2004). Stable Superhydrophobic Coatings from Polyelectrolyte Multilayers.

Zhang, X., Pore, V., Järn, M., Peltonen, J., Vuorinen, T., Levänen, E., & Mäntylä, T. (2007). Effect of Temperature and Film Thickness on the Antireflective Property of Superhydrophobic Boehmite Films Made by the Sol-Gel Technique. , *100*(1), 1407–1412.

Zhang, Y., Ge, D., & Yang, S. (2014). Journal of Colloid and Interface Science Spray-coating of superhydrophobic aluminum alloys with enhanced mechanical robustness. *JOURNAL OF COLLOID AND INTERFACE SCIENCE*, *423*, 101–107. doi:10.1016/j.jcis.2014.02.024

Zhang, Y., Qu, S., Cheng, X., Gao, X., & Guo, X. (2016). Fabrication and Characterization of Gecko-inspired Dry Adhesion , Superhydrophobicity and Wet Self-cleaning Surfaces. *Journal of Bionic Engineering*, *13*(1), 132–142. doi:10.1016/S1672-6529(14)60167-0

Zhang, Y., Wu, J., Yu, X., & Wu, H. (2011). Applied Surface Science Low-cost one-step fabrication of superhydrophobic surface on Al alloy. *Applied Surface Science*, *257*(18), 7928–7931. doi:10.1016/j.apsusc.2011.03.096

Zhang, Y., Yu, X., Zhou, Q., Chen, F., & Li, K. (2010). Applied Surface Science Fabrication of superhydrophobic copper surface with ultra-low water roll angle. , *256*, 1883–1887. doi:10.1016/j.apsusc.2009.10.024

Zheng, Q., & Lü, C. (2014). Size effects of surface roughness to superhydrophobicity. *Procedia IUTAM*, *10*, 462–475. doi:10.1016/j.piutam.2014.01.041

Zhu, M., Zuo, W., Yu, H., Yang, W., & Chen, Y. (2006). Superhydrophobic surface directly created by electrospinning based on hydrophilic material. *Journal of Materials Science*, *41*(12), 3793–3797. doi:10.1007/s10853-005-5910-z

APPENDIX A

1. Image of water droplet on platform of optical angle meter

2. Superhydrophobic water droplet of different sizes on the Al substrate

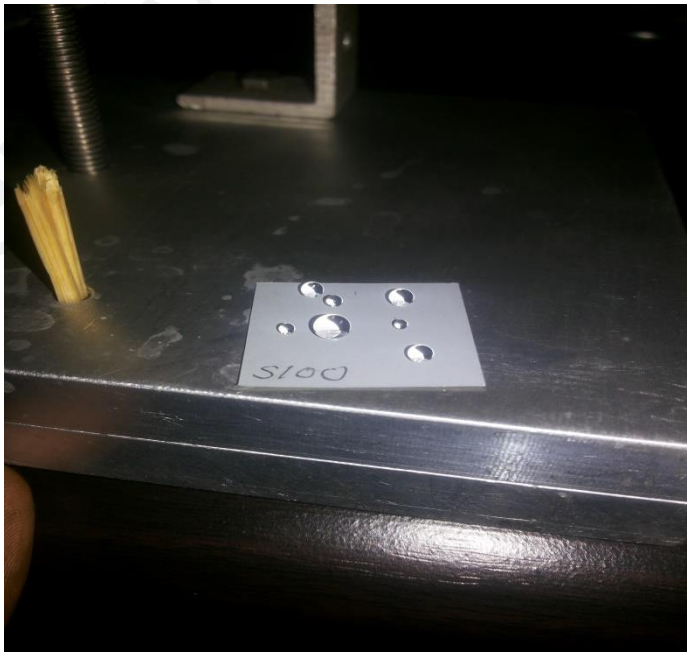

3. Enlarged view of superhydrophobic water droplet of different sizes on the Al substrate